LANGMUIR

pubs.acs.org/Langmuir

Invited Feature Article

Two-Dimensional and Three-Dimensional Ultrathin Multilayer Hydrogels through Layer-by-Layer Assembly

Veronika Kozlovskaya, Maksim Dolmat, and Eugenia Kharlampieva*

Cite This: https://doi.org/10.1021/acs.langmuir.2c00630

Read Online

ACCESS | Metrics & More | Article Recommendations

ABSTRACT: Stimuli-responsive multilayer hydrogels have opened new opportunities to design hierarchically organized networks with properties controlled at the nanoscale. These multilayer materials integrate structural, morphological, and compositional versatility provided by alternating layer-by-layer polymer deposition with the capability for dramatic and reversible changes in volumes upon environmental triggers, a characteristic of chemically cross-linked responsive networks. Despite their intriguing potential, there has been limited knowledge about the structure−property relationships of multilayer hydrogels, partly because of the challenges in regulating network structural organization and the limited set of the instrumental pool to resolve structure and properties at nanometer spatial resolution. This Feature Article highlights our recent studies on advancing assembly technologies, fundamentals, and applications of multilayer hydrogels. The fundamental relationships among synthetic strategies, chemical compositions, and hydrogel architectures are discussed, and their impacts on stimuli-induced volume changes, morphology, and mechanical responses are presented. We present an overview of our studies on thin multilayer hydrogel coatings, focusing on controlling and quantifying the degree of layer intermixing, which are crucial issues in the design of hydrogels with predictable properties. We also uncover the behavior of stratified "multicompartment" hydrogels in response to changes in pH and temperature. We summarize the mechanical responses of free-standing multilayer hydrogels, including planar thin coatings and films with closed geometries such as hollow microcapsules and nonhollow hydrogel microparticles with spherical and nonspherical shapes. Finally, we will showcase potential applications of pH- and temperature-sensitive multilayer hydrogels in sensing and drug delivery. The knowledge about multilayer hydrogels can advance the rational design of polymer networks with predictable and well-tunable properties, contributing to modern polymer science and broadening hydrogel applications.

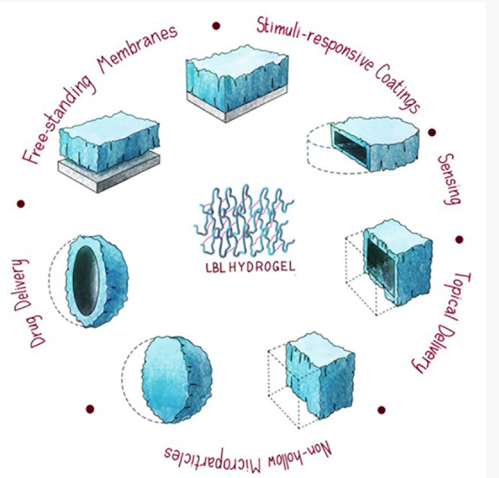

INTRODUCTION

Cross-linked polymeric networks that can absorb large amounts of water (100- to 1000-fold) and host a variety of functional molecules are known as hydrogels and have become critical soft materials for sustainable technologies and biomedicine.[1−4] Hydrogels' ability to mimic human tissue rigidities and model the pathological tissue environment is highly desirable for advanced biomedical applications.[5−7] To mimic tissues' complex hierarchical structures to program varied mechanical and biochemical behaviors, bulk hydrogels made of hydrogel stacks have been developed using polymer layered technologies, including photopolymerization, electrospinning, and sequential physical bonding.[8−10] The pH- and temperature-responsive macromolecules have often been used to develop responsive hydrogels that can change their dimensions and physical properties in a controlled way under external triggers and have been shown to be critical for the controlled delivery of therapeutics and biosensing.[11−14]

For weak polyelectrolyte hydrogels, the acid−base equilibrium is established when the hydrogel is exposed to solutions of varied acidity. The dissociation of charges favors an entropy increase while the charge on the macromolecule chains leads to hydrogel swelling and decreases the entropy of the chains.[15] According to the classic Flory−Rehner model, the gel volume transition in a good solvent is a function of the expansive entropic contributions from polymer−solvent mixing and the retractive elastic forces of polymer chains.[16] The swelling of ionic hydrogels, induced by repulsion between ionized chains and the corresponding osmotic pressure from counterions, is

Received: March 14, 2022
Revised: May 11, 2022

Scheme 1. Multilayer Hydrogels Can Be Synthesized via LbL Polymer Assembly at Planar Surfaces as Surface-Anchored or Free-Standing Coatings and Membranes or via Templating on Sacrificial Nonporous or Porous Particles as Hollow Capsules or Nonhollow Porous Hydrogel Microparticles with Spherical and Nonspherical Shapes[a]

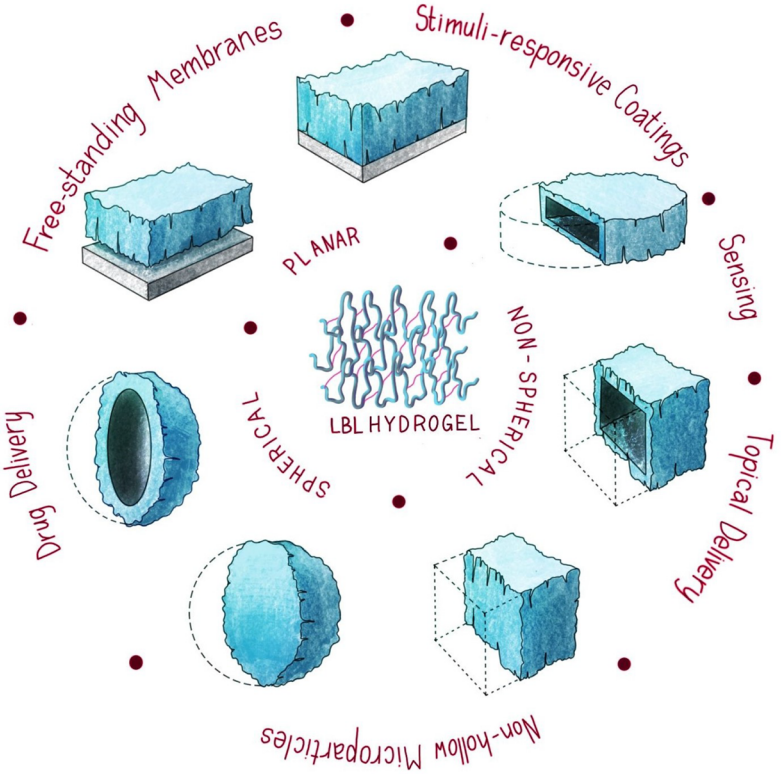

[a]Unique control over multilayer hydrogel properties such as stimuli-induced volume changes, internal architecture, and mechanical properties is allowed by the LbL assembly. These properties are central to developing rapid-response sensing platforms and controlling the encapsulation and release of therapeutics by multilayer hydrogel particles and interactions of the hydrogels with cells and specific targeting and have the potential to advance fundamental and applied knowledge in macromolecular science and biomaterials.

controlled by the solution pH and network cross-link density. The change in solution pH or the addition of salt can result in the screening of the chain charges and cause the shrinking of the hydrogel. The swelling of a polyelectrolyte hydrogel occurs at the pH range around the pK_a of the chain monomer units. Overall, the hydrogel swelling results from the balance among the acid−base equilibrium, the hydrogel's internal structure, and ionic interactions.[17]

Unlike the disadvantageously slow swelling of the millimeter-/micrometer-range bulk hydrogels that can take up to several hours,[18,19] thin responsive hydrogel coatings (~100−1000 nm) with volume-phase transitions triggered by the environmental shifts in pH, temperature, or the chemical surroundings can exhibit a much faster response (within a few minutes or seconds)[20,21] because the swelling rate is inversely proportional to the square of the gel size.[22] Anchoring a hydrogel film to surfaces can also modify the hydrogel swelling behavior. Thus, the swelling of the surface-anchored hydrogels was found to be either larger or smaller than that for free-standing hydrogels of a similar thickness.[23−25]

The thin hydrogels' response time can also be minimized to seconds by creating porosity or decreasing the hydrogel size/thickness.[26,27] Thin hydrogels are often obtained using surface-assisted approaches, including the irradiation of surface-deposited polymer films, photo- and thermal cross-linking of surface copolymer coatings, and surface anchoring of thin hydrogel layers.[28−30]

The recent introduction of thin multilayer hydrogels (<100 nm in dry thickness) based on the layer-by-layer (LbL) self-assembly of polymers has opened new opportunities in the design of nanothin hydrogels with a structural hierarchy.[31,32] The hydrogel architectural hierarchy is introduced when a multilayer hydrogel is made of chemically different stacks, each of stratified layers of cross-linked polymer chains. In contrast to randomly cross-linked hydrogels, this hierarchy allows for greater control over the hydrogel properties.

The multilayer hydrogels can be synthesized when the stepwise deposition of hydrophilic polymers at planar surfaces or on colloidal particles (nonporous, porous; spherical, nonspherical) (Scheme 1) produces the initial multilayer (LbL) coating (Figure 1a,b). The multilayer assembly of polymers can be based on the formation of intermolecular complexes based on covalent, ionic, hydrogen-bonding, $\pi-\pi$, coordination, and guest−host interactions.[33−36] The covalent cross-linking of the physically bound LbL networks results in a hydrogel-like network, termed a multilayer hydrogel, where the polymer chains are linked through covalent bonds and exhibit high swelling by absorbing up to 90 wt % water (Figure 1c).[33,37]

The covalent bonds can exist between the same polymer chains or different polymer components in the multilayer hydrogel.[38] Advantageously, the LbL approach of the multilayer hydrogel fabrication can be translated to various geometries, including two-dimensional (2D) and three-dimensional (3D) substrates with spherical and nonspherical shapes.[39−42] More-

https://doi.org/10.1021/acs.langmuir.2c00630
Langmuir XXXX, XXX, XXX−XXX

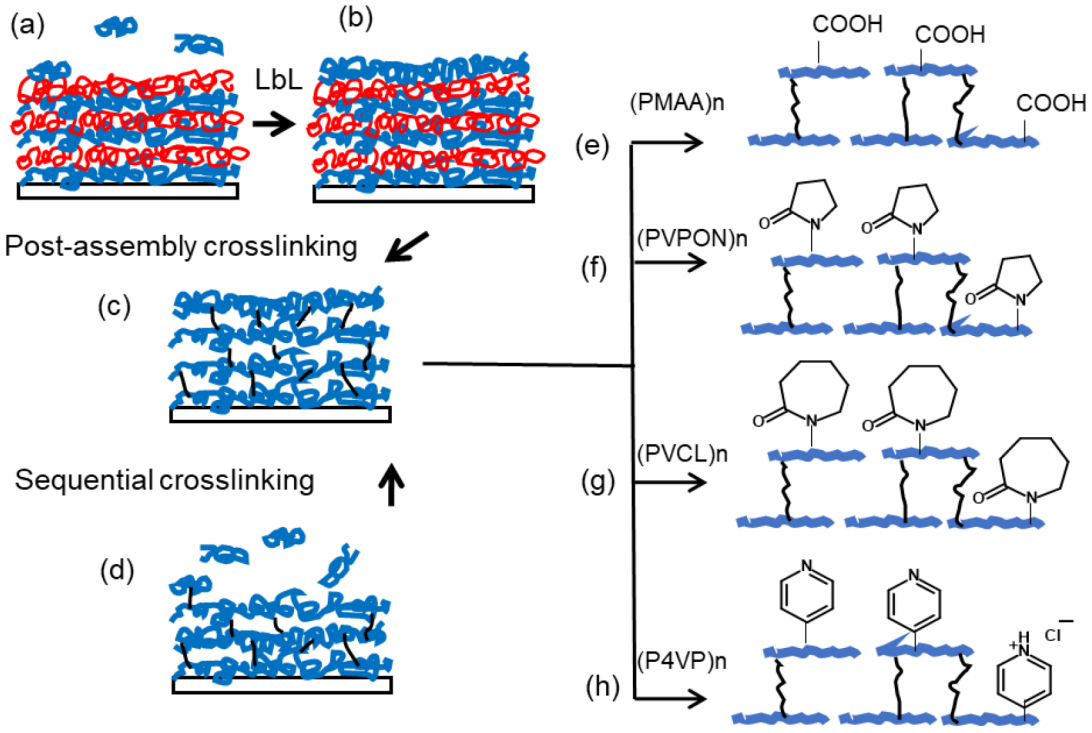

Figure 1. LbL assembly of thin multilayer hydrogels. (a, b) Initial LbL film assembled via the stepwise deposition of polymers at surfaces. (c) Postassembly cross-linking of one or both polymer components with un-cross-linked components released from the multilayer hydrogel. (d) Formation of a single-component multilayer hydrogel via sequential cross-linking during the assembly. Types of thin multilayer hydrogels: (e) anionic, poly(methacrylic acid) (PMAA); (f) nonionic, poly(*N*-vinylpyrrolidone) (PVPON); (g) nonionic, temperature-responsive, poly(*N*-vinylcaprolactam) (PVCL); and (h) cationic, poly(4-vinylpyridine) (P4VP).

over, the multilayer hydrogel thickness can be easily and precisely tuned at the nanoscale by increasing the number of polymer layers during the multilayer assembly,[41] while the varied elasticity can be achieved via varying the cross-linking degree.[43] Unlike polymer brushes or self-assembled monolayers, multilayer hydrogels have a high loading capacity toward functional compounds because of the high surface area, which is particularly valuable for sensing and advanced drug delivery applications.[33]

The hydrogel coatings through the LbL assembly can be obtained via a postassembly cross-linking of the initial polyelectrolyte multilayers or a sequential cross-linking of each polymer layer during the hydrogel assembly (Figure 1d).[31] In the latter case, the multilayer hydrogel is formed through click chemistry reactions or direct covalent reactions between an adsorbed polymer layer and a small cross-linker molecule.[44,45] The ionic (cationic or anionic)[31,37] and neutral[41,46] thin multilayer hydrogels have been demonstrated through the LbL assembly (Figure 1e–h).

Studies on thin multilayer hydrogels are still in their early research stage despite many significant advances. These unique systems have been investigated from various perspectives, including chemical composition, growth mechanisms, and stimuli-triggered swelling/shrinkage.[33,34,47] Our group has contributed to this field with critical knowledge of stimuli-responsive multilayer hydrogels' internal architectures and their solution behavior and developed nonspherical multilayer hydrogel colloids as capsules and hierarchically structured microparticles. In this Feature Article, we highlight our studies on the thin multilayer hydrogels that allowed for resolving the questions of internal layer uniformity and mixing, which are crucial issues in rational hydrogel design, and investigated structural and compositional changes upon the assembly of multilayer hydrogels and their response at the molecular level. We also discuss the construction of hybrid hydrogel materials with "multicompartment" architectures and precisely controlled hydration and temperature responses. Our studies on the multilayer hydrogels demonstrate the effects of the internal architecture of multilayer hydrogels derived from initially well-stratified LbL thin films on their swelling in water, and we discuss the assembly strategies for obtaining highly stratified single and multistack hydrogels. We also uncover the behavior of the stratified multilayer hydrogels in response to environmental stimuli (pH/temperature). We focus on the mechanical properties of the free-standing multilayer hydrogels, including thin films and their closed geometries such as spherical/nonspherical capsules and nonhollow nonspherical hydrogel microparticles, and discuss the applications of the pH- and temperature-sensitive multilayer hydrogels in biosensing and drug delivery.

SYNTHESIS OF TWO-DIMENSIONAL AND THREE-DIMENSIONAL MULTILAYER HYDROGELS

Two-Dimensional Coatings from Multilayer Hydrogels via Spin-Assisted LbL. The spin-assisted LbL mode includes the fast (1–5 s) addition of a polymer solution onto planar surfaces followed by a quick spin of the solution (30–60 s) using a spin-coater. The excess polymer is rinsed off of the surface with a rinse "no-polymer" solution, and the polymer deposition is repeated with a polymer counterpart. Unlike the dipping LbL mode where polymer chains are allowed to diffuse to and adsorb on the surface freely, during the spin-assisted LbL,

https://doi.org/10.1021/acs.langmuir.2c00630
Langmuir XXXX, XXX, XXX–XXX

polymer chains are adsorbed in a "frozen" mobility-limited state without considerable mixing between the neighboring layers.[48] The spin-assisted assembly of multilayer hydrogels from hydrogen-bonded or mixed hydrogen-bonded/ionic multilayers allowed for control over the internal structure (layer stratification and mesh size) and stimuli-responsive properties of ultrathin responsive hydrogel coatings.[37,49−53]

pH-Sensitive Coatings. Nanothin (<100 nm thick) anionic and cationic multilayer hydrogel surface coatings from poly(methacrylic acid) (PMAA, pK_a 5 to 7)[49,52,53] and poly(4-vinylpyridine) (P4VP, pK_a 3.5−4.5)[37] were developed in our group using the spin-assisted LbL (Figure 1e,h). The hydrogel films involving pH-sensitive PMAA networks were mostly produced by the chemical cross-linking of PMAA layers in PMAA/poly(*N*-vinylpyrrolidone) (PVPON) hydrogen-bonded multilayer templates followed by the release of the sacrificial PVPON binder from the PMAA network at pH >7 as a result of PMAA deprotonation. Nanothin P4VP hydrogel coatings were synthesized in aqueous media via the selective cross-linking of water-soluble poly(4-vinylpyridine-*co*-(aminopropyl) methacrylamide) (P4VP-NH_2) copolymer layers within the P4VP/PMAA multilayer.[37]

Temperature-Sensitive Coatings. The temperature-responsive multilayer hydrogel surface coatings were also developed in our group from the LbL assemblies of PMAA and a poly(*N*-vinyl caprolactam-*co*(aminopropyl) methacrylamide) (PVCL-NH_2) copolymer (Figure 1g).[41,46] PVCL is a lower critical solution temperature (LCST) polymer with a continuous coil-to-globule transition at 32−50 °C. PVCL is especially attractive for biomedicine because of its water solubility and hydrophilicity at T < 30 °C and nontoxicity in contrast to poly(*N*-isopropylacrylamide).[11]

Using the PVCL-NH_2 copolymer, we have demonstrated the synthesis of single- and multistrata PVCL multilayer hydrogels (Figure 2).[46] The single PVCL hydrogel stack is synthesized when PVCL-NH_2 random copolymer layers assembled with PMAA via the spin-assisted LbL are cross-linked with glutaraldehyde, and PMAA is released from the network at basic pH. When a hydrophilic PVPON-NH_2 copolymer was additionally used to obtain a PVPON hydrogel stack on the top or bottom of the PVCL hydrogel stack, the double-stack $(PVCL)_n(PVPON)_m$ hydrogel coating was obtained, where the subscripts denote the number of individual polymer layers in a hydrogel stack.[46] This double-strata multilayer hydrogel possesses a structural hierarchy in which each hydrogel stack also has a layered architecture from PVPON or PVCL chains. Unlike random bulk hydrogels, this hierarchy allows for precise control over the coating's properties that are inaccessible in bulk gels, including controlled hydration of a specific part of the hydrogel coating.[46]

We have also developed a thermoresponsive multilayer hydrogel composed of PVCL core−shell nanogel particles (νPVCL).[54] The PVCL nanogels were synthesized through emulsion polymerization and had a shell of the acrylic acid functional group around the PVCL core. The layers of the νPVCL were used instead of the PVCL linear chains in the spin-assisted assembly of the multilayer hydrogel and were cross-linked with either adipic acid dihydrazide (AAD) or ethylene diamine (EDA) cross-linkers. The use of the PVCL nanogels allowed for larger (~3.2-fold) temperature-responsive volume changes of the hydrogel in contrast to those of the hydrogel made of the PVCL linear chains (~2-fold).[54]

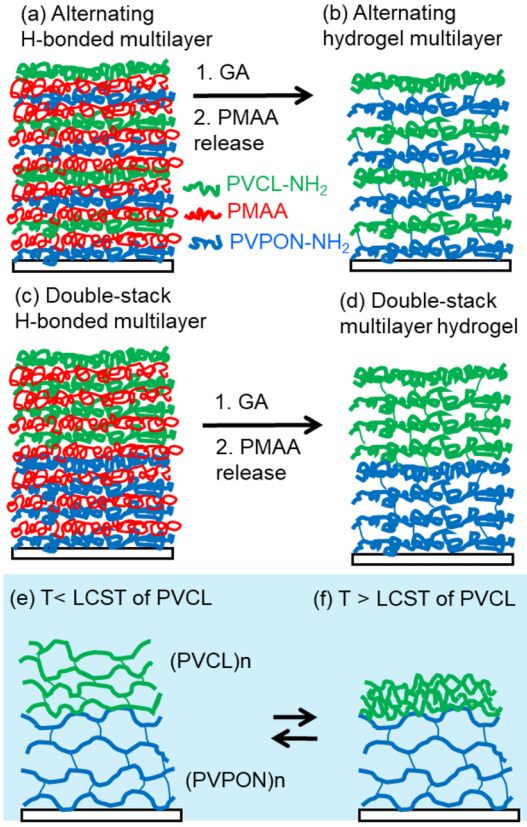

Figure 2. Hydrogen-bonded multilayer of (a) alternating (PVPON-NH_2/PMAA/PVCL-NH_2/PMAA)$_m$ or (c) double-stack (PVPON-NH_2/PMAA)$_n$(PVCL-NH_2/PMAA)$_m$ formed using spin-assisted LbL. After the cross-linking of PVPON-NH_2 and PVCL-NH_2 layers with GA and the release of PMAA, (b) an alternating (PVPON/PVCL)$_n$ or (d) a double-stack (PVPON)$_n$(PVCL)$_m$ multilayer hydrogel is produced. (e) Both hydrogel stacks in the (PVPON)$_n$(PVCL)$_m$ stratum are swollen at T < LCST of PVCL, and (f) the (PVCL)$_n$ hydrogel stack is collapsed at T > LCST. Reproduced with permission from ref 46. Copyright 2016 American Chemical Society.

Free-Standing Hydrogel Films. Sensors and lab-on-a-chip systems often require substrate-free materials and can benefit from free-standing hydrogels.[55−58] Accounting for their nanoscale thickness, lifting thin hydrogels from a template is challenging because of their mechanical fragility. Thin multilayer films are typically released using dry peeling or sacrificial layer approaches.[59−62] Although the first method works for micrometer-sized films,[59,63] the other requires a trigger to dissolve the sacrificial layer, such as pH, ionic strength, temperature, or solvent variation, which could change the film morphology, composition, and thickness.[64−68]

Our group has recently developed a versatile and straightforward lift-off approach to obtain nanothin free-floating PMAA hydrogels by dissolving a thick sacrificial SiO_2 sublayer (Figure 3).[39] Hydrogels (~100 nm dry thickness) were released from silicon templates by etching an (~300 nm) underlying silica layer with a mixture of hydrofluoric acid and NH_4F at pH 5.[39] The AFM measurements demonstrated no changes in the thickness, morphology, and mechanical properties of the lifted hydrogel coatings of highly hydrated $(PMAA)_{60}$ networks (~80% hydration at pH 5). Two-fold thinner $(PMAA)_{30}$ hydrogels (~60 nm dry thickness) were also successfully released and transferred to Si wafers after being reinforced

https://doi.org/10.1021/acs.langmuir.2c00630
Langmuir XXXX, XXX, XXX−XXX

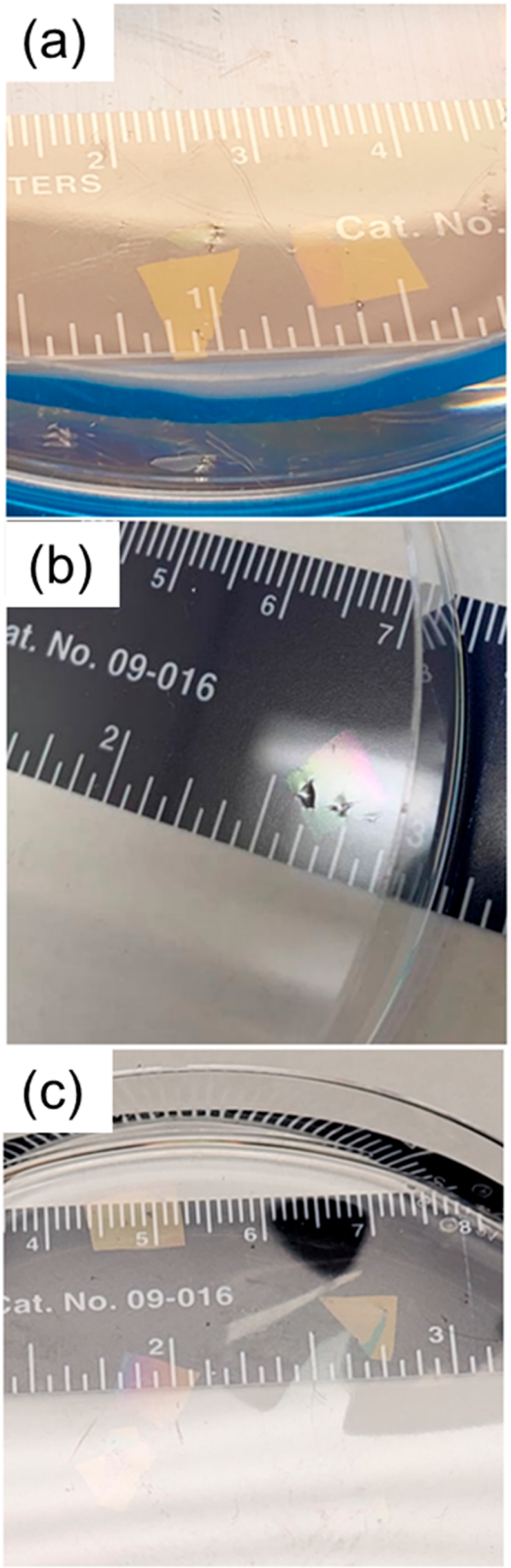

Figure 3. Optical images of (a) free-floating 16 h cross-linked $(PMAA)_{60}$ hydrogels, (b) $(PMAA)_{60}$-Zr(IV) hydrogels, and (c) 8 h cross-linked $(PMAA)_{60}$ hydrogels at pH 5. The upper scale is in centimeters. Reproduced with permission from ref 39. Copyright 2021 American Chemical Society.

with Zr(IV) ions, while the ion-free hydrogel was less mechanically robust and could not be easily transferred to another substrate.[39]

Synthesis of Colloids from Multilayer Hydrogels. The template-assisted multilayer hydrogel assembly allows the fabrication of hollow capsules of varied size, geometry, and thickness with a multilayer hydrogel shell.[39,43] The hydrogel shell is stabilized through the covalent links between the polymer layers when the particle template is dissolved, and available functional groups provide the stimuli-responsiveness of the hydrogel shell.[41,43] After the core dissolution, the hydrogel shell swells because of the increased osmotic pressure, and the hydrogel rigidity opposes the swelling. Both the critical pressure difference and the stiffness of the multilayer hydrogel can control capsule deformation and are dependent on the shell thickness and the capsule size.[69]

Decreasing the rigidity of polymeric colloids to the kPa range has been shown earlier to increase particle circulation *in vivo*[70] and improve particle accumulation by target tissues.[71] Conversely, a nonspherical shape of a hydrogel particle has been demonstrated to favor the particle passing through pores and channels with smaller-than-particle-size diameters.[45] In our work on the multilayer hydrogel capsules, we have demonstrated that despite the inherent softness and high swelling of the capsule wall, the nonspherical multilayer hydrogel capsules with the shape of nonspherical template particles can be obtained after template dissolution.[43,72,73]

Nonspherical Multilayer Hydrogel Capsules. We showed that the rigidity of the hydrogel capsule shell is crucial to maintaining the initial shape of the template after the core dissolution with the ultrathin capsule wall (<50 nm) and the highly hydrated state of the hydrogel network (up to 80% water by volume). The cubical PMAA multilayer network capsules were synthesized as hydrogel replicas of cubic $MnCO_3$ microparticles (4 to 5 μm) through the chemical cross-linking of hydrogen-bonded multilayer films of PMAA and PVPON.[74] Single-component $(PMAA)_{20}$ capsules with a 20-layer hydrogel wall were produced either by cross-linking PMAA layers with a bifunctional cross-linker or by using a PMAA-NH_2 copolymer assembled with PVPON, where PMAA-NH_2 layers were covalently bound through carbodiimide-assisted cross-linking, resulting in amide linkages between amino and carboxylic groups and followed by PVPON release at basic pH.[43,73] The two-component $(PMAA\text{-}PVPON)_5$ hydrogel capsules were obtained when PVPON-NH_2 was assembled with PMAA followed by the carbodiimide-assisted binding of PMAA to PVPON-NH_2 layers.[43] Using discoid silicon microparticles with a large aspect ratio as sacrificial templates led to the discoidal hydrogel capsules, either single- or two-component, with the shape of a red blood cell, an erythrocyte.[72]

Stimuli-Induced Changes in Hydrogel Capsules. The hydrogel chemistry, solvent affinity, and cross-link density dictate the responsive behavior of the multilayer hydrogel capsule's wall. The spherical capsule made of cross-linked PMAA undergoes reversible sharp volume transitions by ~2-fold swelling in response to a pH increase, leading to swollen, thermodynamically stable microstructures.[31,43] Unlike bulk gels, the capsule hydrogel wall exhibits a fast volume increase in response to the external stimuli in which the hydrogel microcapsule has a much larger free volume due to the capsule's interior.

For spherical PMAA hydrogel capsules, the size increase at pH >6 due to the capsule shell swelling increased the overall volume

https://doi.org/10.1021/acs.langmuir.2c00630
Langmuir XXXX, XXX, XXX−XXX

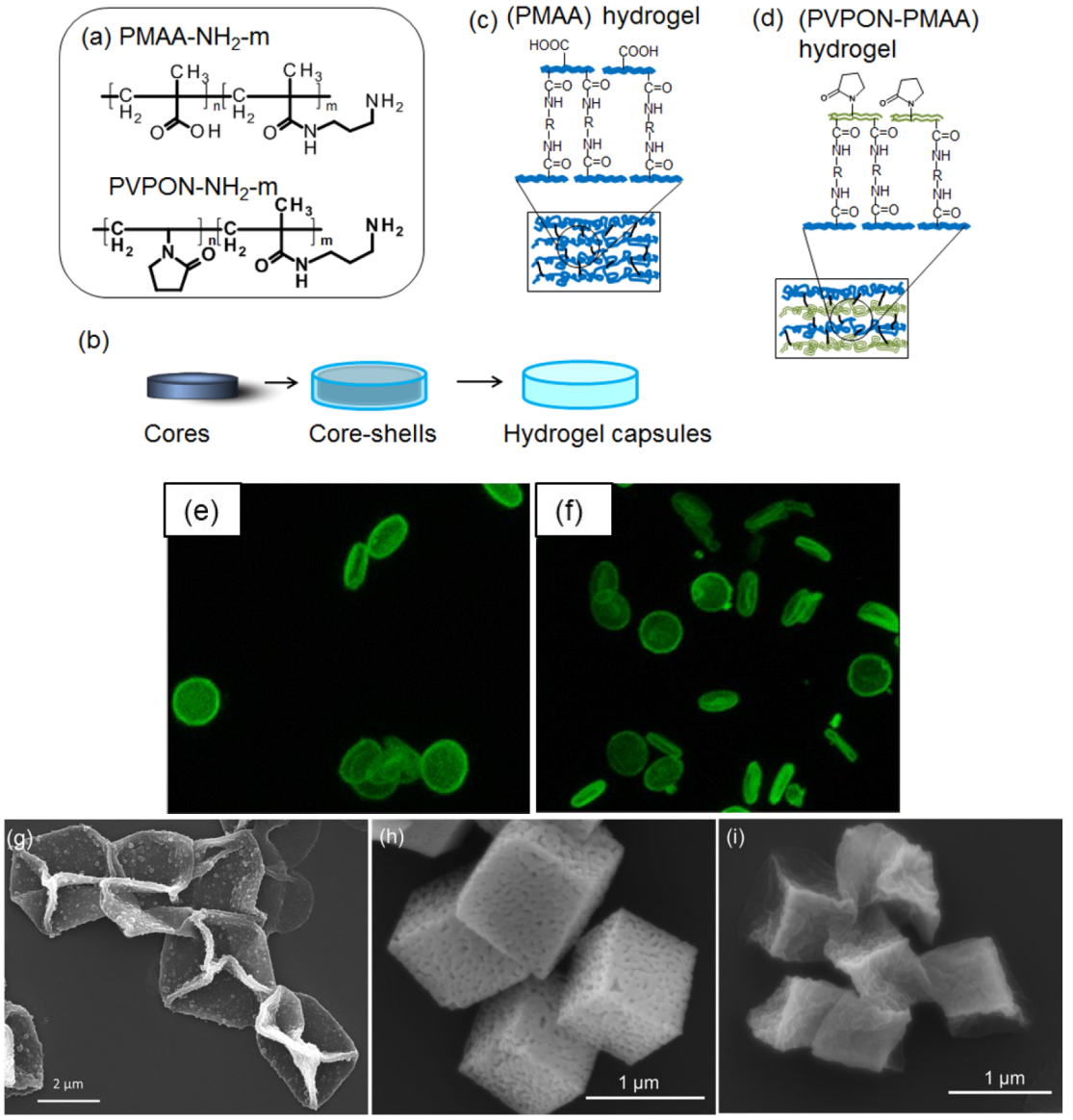

Figure 4. (a) Poly(methacrylic acid-*co*-(aminopropyl)methacrylamide) (PMAA-NH_2) and poly(*N*-vinylpyrrolidone-*co*-(aminopropyl)methacrylamide) (PVPON-NH_2) copolymers used for capsule fabrication. (b) Synthesis of single- and two-component hydrogel capsules of (c) (PMAA) and (d) (PMAA-PVPON) obtained from hydrogen-bonded (PMAA-NH_2/PVPON) and (PVPON-NH_2/PMAA) multilayers, respectively, via carbodiimide-assisted cross-linking. Confocal microscopy 3D images of (e) (PMAA-PVPON) multilayer hydrogel capsules swollen at pH 7.4 from (f) biconcave (PMAA-PVPON) multilayer hydrogel capsules deswolllen at pH 4. Reproduced with permission from ref 72. Copyright 2014 American Chemical Society. (g) SEM image of cubical $(PVCL)_{15}$ hydrogel capsules. Reproduced with permission from ref 41. Copyright 2012 American Chemical Society. (h) SEM images of a porous manganese oxide template of 700 nm and (i) their (PMAA) multilayer hydrogel cubical replicas of 500 nm. Reproduced with permission from ref 78. Copyright 2018 American Chemical Society.

of the spherical capsules, similar to Donnan swelling in ionic gels.[31] The correlation between the pH-triggered swelling of the capsule wall and the capsule size expansion has not been addressed, although it is generally assumed that a spherical PMAA capsule wall exhibits the same thickness response as the corresponding surface-anchored hydrogel.[31] We found that while spherical capsules exhibited a uniform stress distribution during reversible isotropic swelling, nonspherical hydrogel capsules demonstrated a more complex capsule volume change leading to the overall anisotropic shape. Thus, for example, the cubical $(PMAA)_{13}$ hydrogel capsules exhibited anisotropic pH-induced swelling in which the cubical faces bulged outside, resulting in a quasi-spherical shape transformation.[43,74] Conversely, isotropic swelling was observed for the two-component cubical $(PMAA\text{-}PVPON)_5$ hydrogel capsules in which only the capsule size increased along with the preserved cubical shape, similar to that for the spherical hydrogel capsules in basic pH solutions.[43]

For discoidal anionic $(PMAA)_{15}$ and $(PMAA\text{-}PVPON)_5$ hydrogel capsules (Figure 4a–c), an increase in the basic pH resulted in various degrees of out-of-plane swelling of the discoidal circular faces (i.e., circular face bulging) (Figure 4e,f).[72] Conversely, the spherical $(PMAA)_{15}$ capsules displayed an enormous 19-fold volume increase only when the pH increased from 4 to 7.4.[72] In contrast to those, the two-component $(PVPON\text{-}PMAA)_5$ capsules underwent only a 2.9-fold volume increase. This difference in the pH-triggered variations in capsule volume was rationalized through the

https://doi.org/10.1021/acs.langmuir.2c00630
Langmuir XXXX, XXX, XXX−XXX

different free volumes within the capsule hydrogel shells. The $(PMAA)_5$ multilayer hydrogel displayed a 2-fold greater water uptake than $(PMAA\text{-}PVPON)_5$ at pH 3 with water contents of 41 and 19% found for $(PMAA)_5$ and $(PMAA\text{-}PVPON)_5$, respectively.[72] Therefore, the presence of the second component, PVPON, reduced the free volume in the two-component network, thereby suppressing the capsule softness and swelling.[72]

Moreover, the pH-triggered dimensional changes of $(PMAA)_{15}$ and $(PMAA\text{-}PVPON)_5$ discoidal hydrogel capsules were considerably different.[72] Both the radial and axial dimensions of (PMAA) capsules were 1.8-fold greater than those observed for $(PMAA\text{-}PVPON)_5$ capsules at pH 7.4. The more significant expansion of the one-component hydrogel discoids was consistent with the more expansive swelling of the corresponding hydrogel spheres and the surface-attached hydrogel films compared to their two-component counterparts. However, the aspect ratios of the two types of discoidal capsules at pH 7.4 remained similar, indicating that both hydrogel capsules expanded similarly. Those aspect ratios were smaller than the aspect ratio for their solid templates, indicating the preferential expansion in the axial direction for both types of capsules upon core dissolution and exposure to the neutral pH.[72]

Excitingly, the basic pH-triggered increase in the discoidal capsule volume resulted in anisotropic swelling/shrinkage leading to the discoidal-to-ellipsoidal shape transformations with the degree of this shape transitions depending on the wall composition.[72] The pH-triggered changes in the aspect ratios for the two types of discoidal hydrogel capsules were attributed to a greater degree of out-of-plane swelling for (PMAA) capsules compared to that of (PVPON−PMAA) at pH 7.4.[72]

We also explored the effect of temperature on the volume changes of cubical multilayer hydrogel capsules obtained from a thermoresponsive PVCL-NH_2 copolymer (Figure 4g).[41] The cubical capsules with a single-component PVCL multilayer hydrogel shell were synthesized by the glutaraldehyde-assisted cross-linking of PVCL-NH_2 copolymer layers within the PVCL-NH_2/PMAA hydrogen-bonded network followed by the release of PMAA at basic pH. Both spherical and cubical PVCL hydrogel capsules decreased in volume/size at the solution temperature elevation from 25 to 50 °C. Although both capsule shapes demonstrated similar shrinkage ratios of ∼20%, the cubical capsules, despite their sharp edges and vertices, showed remarkable shape maintenance during the capsule shrinkage. This anisotropic volume change with the preserved cubical shape was attributed to the higher rigidity of the PVCL chain, unlike the PMAA in PMAA hydrogel cubical capsules cross-linked with ethylenediamine.

Nonhollow Multilayer Hydrogel Microparticles. The multilayer hydrogel assembly within the pores of porous sacrificial templates allowed for synthesizing the multilayer hydrogel microparticles with the hierarchical nanostructure (Figure 4h,i).[75−78] In contrast to hollow multilayer hydrogel capsules, the PMAA hydrogel particles were obtained as the inverse replicas of the porous manganese oxide template where the thin PMAA multilayer hydrogel film is "packed" throughout the particle volume. This structure provides a large surface area for the interaction with functional molecules and chemical reactions. Additionally, the PMAA multilayer structure of the hydrogel coating provided a quick, within seconds, and completely reversible response to increasing pH. In this case, the size of the PMAA hydrogel particle could quickly increase by 70% at the pH increase from 5 to 7.5.[75,76] The bottom-up hierarchical morphology of the cubical PMAA hydrogel microparticles provided the stability of their cubical shape both in solution upon pH-induced volume changes and, more remarkably, in the dry state upon complete particle dehydration.[77,78]

PROPERTIES OF MULTILAYER HYDROGEL COATINGS AND COLLOIDS

Stimuli-Induced Volume Changes in Hydrogel Planar Coatings. We found that the degree of pH-induced swelling of multilayer PMAA hydrogels can be controlled by controlling the interlayer mixing from well stratified to highly intermixed by changing the assembly conditions from the spin-assisted to dipped LbL (Figure 5a,b).[49,52,53] The spin-assisted multilayer

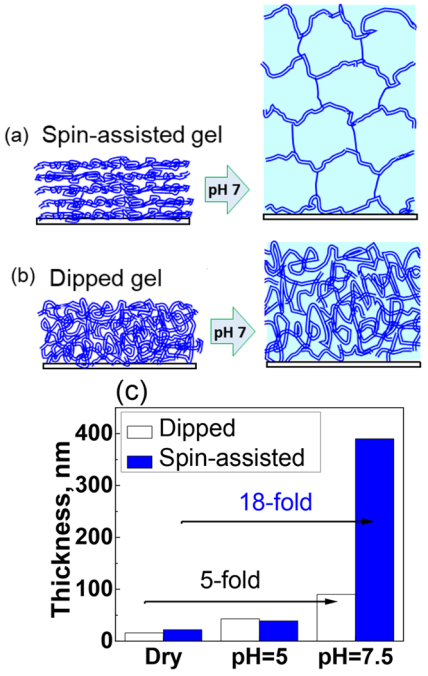

Figure 5. Swelling of (a) spin-assisted and (b) dipped hydrogels at pH ≥7. (c) Thicknesses of spin-assisted (filled) and dipped (open) hydrogels in dry states and in solutions at pH 5 and 7.5. Reproduced with permission from ref 49. Copyright 2013 American Chemical Society.

hydrogel surface-anchored coatings of 20−40 nm exhibited a dramatic 10-fold increase in thickness when transitioned between pH 5 and 7.5, unlike the 2-fold swelling observed in less-organized hydrogels of the same thickness made through the dipped LbL (Figure 5c). This different degree of swelling is due to the large loops and fewer chain entanglements produced during the spin-assisted assembly that expanded at high pH, providing the needed free volume for swelling.[49,52] In contrast, the much lower swelling at basic pH in the dipped multilayer hydrogels is due to polymer chains that are more interdiffused in the dipped hydrogel coatings because of chain exchanges during assembly. This chain interdiffusion decreases the free volume in the dipped hydrogels, significantly constraining the multilayer hydrogel swelling.

Similarly, the positively charged (P4VP) multilayer hydrogel coatings were shown to undergo large 10-fold swelling because of the polymer layer stratification when the pH was decreased to the acidic range. Remarkably, when the P4VP hydrogel shrinks

https://doi.org/10.1021/acs.langmuir.2c00630
Langmuir XXXX, XXX, XXX−XXX

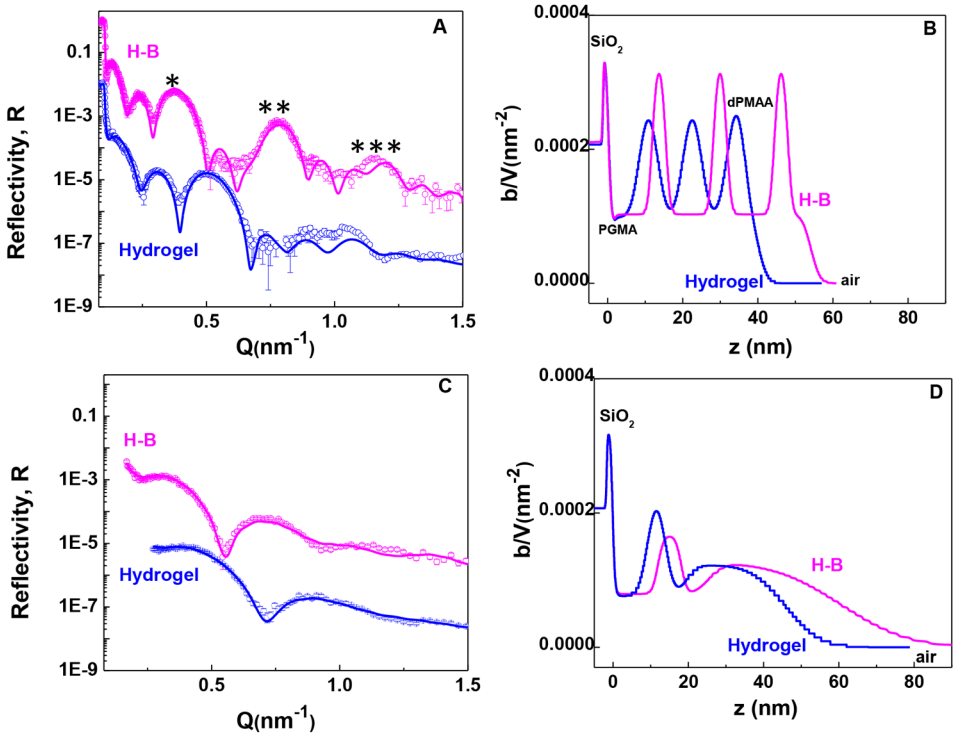

Figure 6. (A, C) NR and (B, D) fitted SLD profiles for dry H-bonded (H-B) (A, B) SA and (C, D) dipped films and the corresponding hydrogels (Hydrogel) on silicon wafers. (A) The first-, second-, and third-order Bragg peaks are shown with asterisks in the NR profile. (B) The SLD profiles illustrating contrasting and periodic dPMAA peaks follow the SiO_2 peak and PGMA precursors' shallow dip. Reproduced with permission from ref 53. Copyright 2020 American Chemical Society.

at pH >5, water is pushed out of the thin hydrogel film, and the hydrogel's thickness is decreased to that for the dry state.[37] These P4VP or PMAA multilayer hydrogels obtained through the spin-assisted LbL are exceptional examples of an ultrathin but highly swollen coating capable of a substantial volume change in response to opposite pH variations.

Comparing the temperature-responsive multilayer hydrogels made from the layers of PVCL linear chains or the νPVCL nanogels showed that both types of layered hydrogels reversibly decreased in thickness as the solution temperature increased from 25 to 50 °C.[41,54] The degree of shrinkage was similar for both coatings and varied from 1.8- to 3.2-fold depending on the cross-linker and hydrogels' cross-link densities. However, the inclusion of νPVCL core−shell nanogels as layers within the multilayer coating allowed for a much more significant 9-fold increase in their thickness at pH 7.4 and 25 °C with 90 wt % water intake, unlike the moderate swelling of 2.6-fold for the hydrogel synthesized from PVCL linear chains.[54] The hierarchical structure of the νPVCL-based multilayer hydrogel also allowed for the inclusion of different functional molecules in the νPVCL depots within the hydrogel coating.[54]

Internal Architecture of Multilayer Hydrogel Coatings. Controlling the internal structure of multilayer hydrogels is among the most challenging tasks in surface polymer chemistry, mainly because of the nanoscale level of the materials. Compared to traditional parameters of hydrogel films, such as the chemical composition, charge balance, thickness, and cross-link density, the control of the internal architecture has been much less explored.[33] Nevertheless, network organization at the nanoscale can regulate hydrogel responsiveness to external stimuli to a degree hardly possible for random networks, which is essential for microfluidics, sensing, and actuation.[79−81] In addition, tuning the internal hydrogel hierarchy would also advance therapeutic applications of multilayer hydrogels in medical devices, controlled delivery, and tissue regeneration.[81]

Films made of ionically paired polyelectrolytes with individual layer thicknesses of several nanometers were shown with neutron reflectivity to have well-defined stratification with intermixing between adjacent layers of the same order as the layer thickness.[82−86,96] The evidence of internal layering was also observed in some hydrogen-bonded films.[91,91] For thin multilayer hydrogel films, the fundamental significance of such studies lies in understanding the polymer design and assembly strategies for resulting hydrogel architectures. Although the internal structure has been shown to influence the properties of bulk hydrogels,[9,87] the internal structure of thin films remains less explored mainly because of the lack of deuterated polymers and limited access to neutron reflectometry.[88−93] Another limitation is caused by insufficient data analysis tools that allow quantitative parameter retrieval in the systems changing the composition and internal structure due to physical/chemical modifications.

pH-Responsive Coatings. One of the unique features of multilayer hydrogels is that one can select a multilayer composition. In this case, selectively deuterated layers can be used to show layer distribution within the film in dry and hydrated states and how postassembly treatments can control the internal layering.[94−99] Neutron contrast in the initial hydrogen-bonded PMAA/PVPON coatings was provided by depositing deuterated PMAA (dPMAA) in every fifth bilayer.[49,52,53] In this case, a chemical cross-linking of PMAA layers and subsequent PVPON release resulted in a single-component PMAA hydrogel with three dPMAA marker layers. The quality of layer organization was studied by analyzing the

https://doi.org/10.1021/acs.langmuir.2c00630
Langmuir XXXX, XXX, XXX−XXX

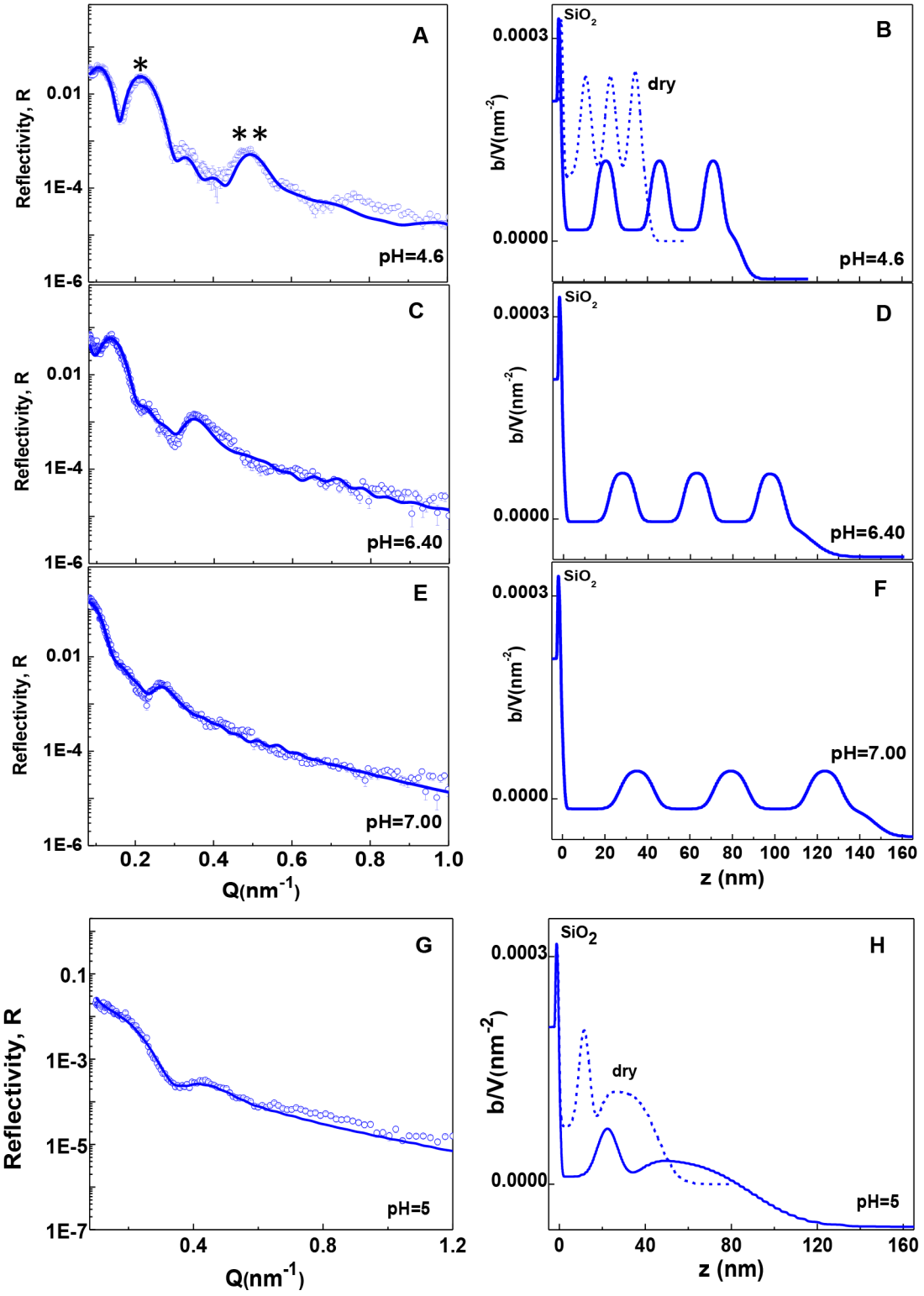

Figure 7. (A, C, E, and G) NR data and (B, D, F, and H) corresponding SLD profiles for an SA hydrogel hydrated at (A–F) pH 4.6, 6.4, and 7.0 and dipped hydrogels hydrated at (G, H) pH 5. (A) The first- and second-order Bragg peaks in the NR profile for the SA network are illustrated by one and two asterisks, respectively. The SLD profiles of the SA and dipped hydrogels in dry states are shown by the dashed lines in the B and H panels, respectively. Reproduced with permission from ref 53. Copyright 2020 American Chemical Society.

spacing between deuterated layers as reflected in superlattice peaks in the NR profiles when the normalized NR was plotted against wavevector transfer, Q (Figure 6A,C).[53] The corresponding scattering-length density (SLD) profile, obtained by fitting the NR data, provided the thickness of the individual dPMAA layers, the distance between them, the total film thickness, and the extent of layer intermixing expressed through the internal roughness (Figure 6B).

https://doi.org/10.1021/acs.langmuir.2c00630
Langmuir XXXX, XXX, XXX−XXX

NR showed that the architecture of PMAA networks was dictated by the internal structure and composition of the initial PMAA/PVPON multilayers.[52,49] One approach to controlling network organization includes varying the deposition conditions used to assemble (PMAA/PVPON) templates. The layer organization varied from well-stratified to highly intermixed for the networks derived from spin-assisted and dipped H-bonded templates, respectively.[49,53] Spin-assisted hydrogels preserved the initial periodicity of dPMAA layers found in their hydrogen-bonded precursors as indicated by sharply contrasting and equally spaced deuterated layers in the hydrogel SLD profiles (Figure 6B).[53] A partial decrease and the corresponding increase in the average thickness of dPMAA after cross-linking indicated the enhanced intermixing and diffusion of dPMAA with protiated material (Figure 6B). Unlike a persistent well-defined layering in the spin-assisted hydrogen-bonded films, their dipped counterparts revealed a highly disordered structure with rapidly decaying layering away from the substrate as reflected in a gradual decrease in peak height and increased broadening (Figure 6D). Cross-linking the dipped films further enhanced layer intermixing and resulted in almost a complete loss of layered structure away from the substrate (Figure 6D).

Another parameter impacting the internal hydrogel structure is the molecular weight of PVPON, a sacrificial binder released upon chemical cross-linking of PMAA layers. We found that hydrogen-bonded films assembled with 2.5 kDa PVPON showed a larger distribution of dPMAA compared to that for PVPON of 55 and 360 kDa, which could be explained by the higher mobility of the short-chain PVPON. Cross-linking of the film revealed the opposite effect.[52] The deuterated layers were distributed more widely in the hydrogels templated with higher-molecular-weight PVPON, suggesting more pronounced intermixing of PMAA chains upon cross-linking. Importantly, all three networks showed a high degree of stratification, indicating that PVPON release did not disturb the layering.[52]

Finally, we found that spin-assisted hydrogels preserved well-organized layering upon hydration when the solution pH ranged from 4.6 to 7.0 with the preserved original placement of dPMAA (Figure 7A–F), unlike highly intermixed dipped films featuring rapid layer decay with the distance from a substrate (Figure 7G,H).[53] We found that the extent of layer intermixing within spin-assisted films increased from three to five PMAA layers in dry hydrogen-bonded and hydrogel films, respectively (Figure 8A,B).[53] Upon exposure to pH 4.86, the network swells to twice its dry thickness, decreasing the penetration of PMAA into neighboring layers (Figure 8C). Structural features were defined by comparing the swelling ratios of the entire hydrogel film and individual dPMAA layers. While the entire hydrogel film exhibited 3.8-fold swelling at pH 7, the dPMAA layer swelled only 3.4-fold, indicating nonuniform network swelling. The differential expansion was attributed to alternating the cross-link-poor and cross-link-rich areas featuring 10.0 and 5.8 monomer units between cross-links, respectively (Figure 9).[53]

We developed a highly constrained, self-consistent, mass-balanced model and applied it to NR data from dipped and spin-assisted hydrogels to extract accurate quantitative information about the film's internal structure, including the degree of layer interpenetration in dry and hydrated states.[53] This model accounts for changes in mass density and film stoichiometry wherein the amount of initially deposited PMAA is preserved upon chemical cross-linking and subsequent hydration. Specifically, using ellipsometry to determine thicknesses and

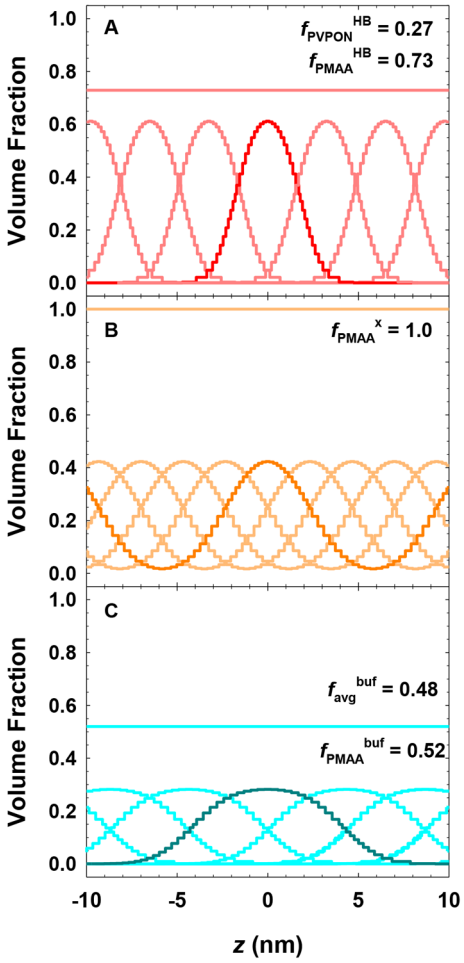

Figure 8. PMAA distribution within the H-bonded film (A) before and after cross-linking in (B) dry and (C) hydrated states. The deuterated and protiated PMAA layers are shown in darker and lighter colors, respectively. The initial H-bonded film in (A) is composed of 0.73 PMAA (f_{PMAA}) and 0.27 PVPON (not shown). The cross-linked film in (B) decreased in total thickness after PVPON release, resulting in more interdiffused PMAA layers. This cross-linked film is hydrated at (C) pH 4.86 and features 0.48 and 0.52 volume fractions for the buffer solution (f_{avg}^{buf}) and PMAA (f_{PMAA}^{buf}), respectively. Reproduced with permission from ref 53. Copyright 2020 American Chemical Society.

corresponding amounts of PMAA and PVPON deposited in each step, a fit model for hydrogen-bonded templates was constructed to include the thickness of marker layers, the mass density, the spacing between marker layers, the internal interfacial widths of the marker layers, and the surface roughness. This model was further applied to dry and hydrated cross-linked films considering that PVPON was driven entirely off, and all PMAA remains after cross-linking. The stoichiometry, mass density, and structure of the pre- and post-cross-linked films were defined by accounting for the change in film stoichiometry upon reaction with the cross-linker followed by self-consistently refining the NR fits to the as-deposited and cross-linked data sets.[53] Final fits for all films were optimized on the basis of the AFM surface roughness and average values of silicon oxide layer thickness among various pH solutions. This model provides quantitative information about the structural parameters of dry and hydrated multilayer hydrogel coatings with selectively labeled film components and the extent of layer interdiffusion. In addition, this approach offers a template that

https://doi.org/10.1021/acs.langmuir.2c00630
Langmuir XXXX, XXX, XXX−XXX

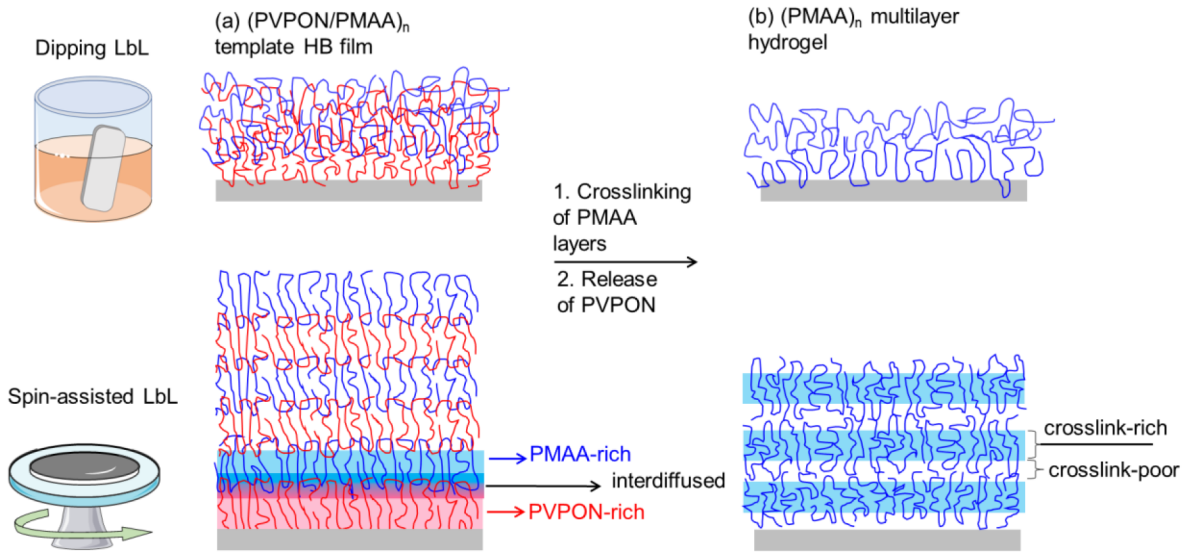

Figure 9. Dipping and spin-assisted LbL methods are applied to produce (a) the initial H-bonded $(PVPON/PMAA)_n$ multilayer (HB), which was converted to (b) a $(PMAA)_n$ multilayer hydrogel by cross-linking PMAA layers followed by PVPON release at pH 8. H-bonded films deposited with an SA LbL method feature partially interdiffused layers between PMAA-rich and PVPON-rich (aka PMAA-poor) strata. Releasing PVPON from cross-linked films leads to PMAA hydrogels with the corresponding cross-link-rich and cross-link-poor areas (bottom right). Reproduced with permission from ref 53. Copyright 2020 American Chemical Society.

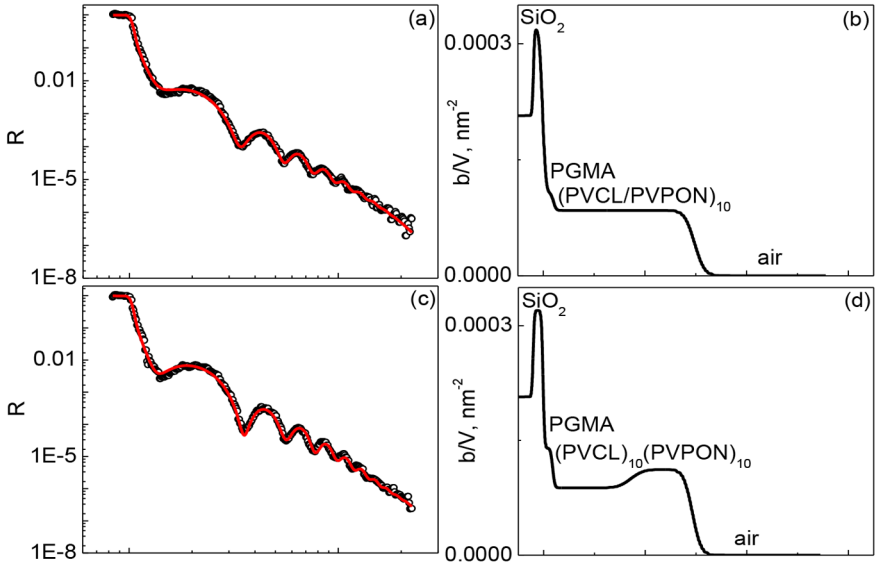

Figure 10. NR data (left panels) and corresponding SLD profiles (right panels) for (a, b) spin-assisted dry alternating $(PVCL/PVPON)_{10}$, (c, d) double-stack $(PVCL)_{10}(PVPON)_{10}$ hydrogels. Open symbols and solid lines show the NR data and fit, respectively. Reproduced with permission from ref 46. Copyright 2012 American Chemical Society.

can be used in NR data analysis whenever tracking the chemical and physical evolution of conserved material quantities is essential.

Temperature-Responsive Coatings. An alternative approach to provide neutron contrast is deuterium-containing solvents (e.g., D_2O). In this case, the contrast is achieved between the nonlabeled polymeric film and the solvent, allowing one to resolve the polymer structure and the distribution of solvent within the multilayer hydrogel.[92] The amount of deuterated water absorbed by nondeuterated polymer chains has been used to determine various film properties such as the thickness and hydration from the difference in scattering density.[100,101] For example, using *in situ* NR, it was possible to discern the individual strata of a nonionic double-stack multilayer hydrogel to determine the effect of internal layering on hydrogel swelling based on the swollen thicknesses of the individual stacks.[46] NR revealed that the $(PVPON)_n(PVCL)_m$ hydrogel double-stack networks are well stratified in both dry and hydrated states, as was evidenced by two distinct (PVPON) and (PVCL) strata of higher and lower scattering density, respectively (Figure 10).[46] In contrast, the $(PVCL/PVPON)_n$ hydrogel synthesized by the alternative deposition of layers exhibited homogeneous SLD profiles indicating a highly mixed structure. The NR measurements also showed that the hydration of these networks was controlled by the stack thickness, stacking order, and solution temperature. The water content consistently increased with the

https://doi.org/10.1021/acs.langmuir.2c00630
Langmuir XXXX, XXX, XXX−XXX

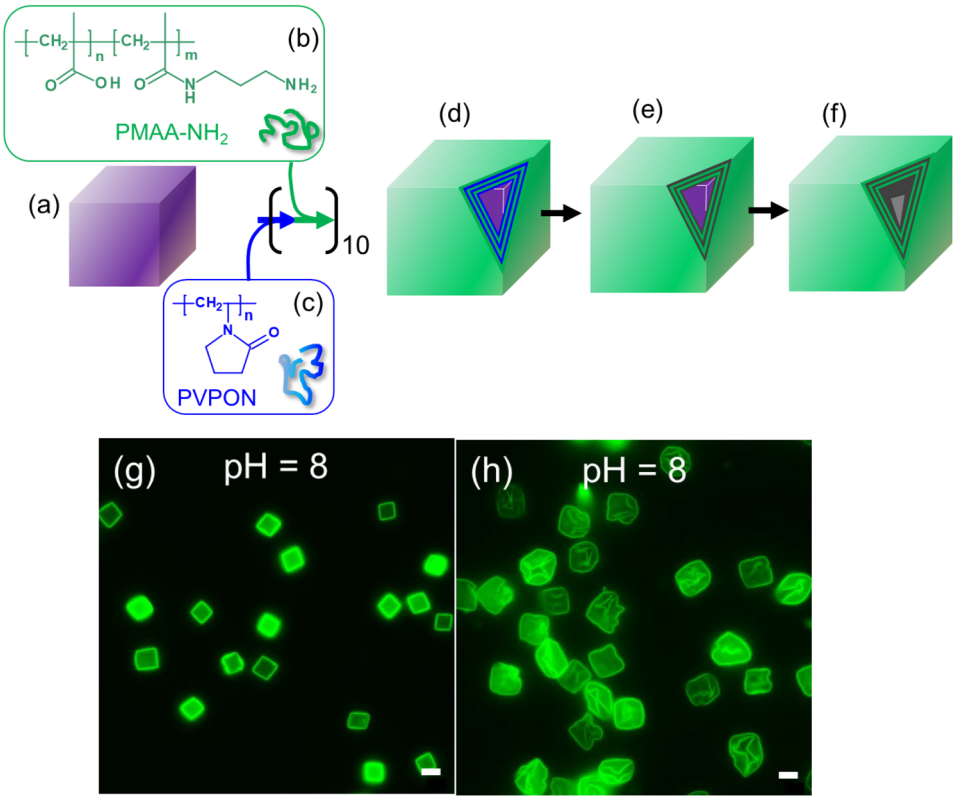

Figure 11. Assembly of cubical (PMAA) multilayer hydrogel capsules. Inorganic cubical cores (a) were stepwise exposed to solutions of (b) PMAA-NH_2 and (c) PVPON at pH 2. (d) Hydrogen-bonded $(PMAA\text{-}NH_2/PVPON)_{10}$ cubical core−shells were cross-linked, and (e) PVPON layers were released at pH 8, leaving behind (f) hollow $(PMAA)_{10}$ multilayer hydrogel cubical capsules after core dissolution and EDTA treatment. Optical fluorescence microscopy images of (g) 10-layer PMAA* and (h) PMAA** multilayer hydrogel capsules assembled from PMAA-NH_2-6.4 and PMAA-NH_2-2.5 copolymers, respectively, are shown at pH 8. The scale bar is 10 μm in both images. Reproduced with permission from ref 73. Copyright 2021 American Chemical Society.

amount of hydrophilic PVPON in the network, resulting in suppressed temperature-induced shrinkage, while the magnitude of temperature-based shrinking increased with the PVCL thickness. Heating the PVCL to above the LCST resulted in a greater decrease in film thickness if the PVCL was included as a bottom stratum. In contrast, a suppressed hydrogel shrinkage with a lower degree of temperature-induced film thickness was found when the PVCL was deposited on top of PVPON.[46] The suppressed temperature response in the latter case can be attributed to hydrophilic bulk water above the top stratum.

Thus, the NR showed that the degree of pH-induced swelling of multilayer PMAA hydrogels can be controlled by regulating their internal structure from well stratified to highly intermixed using spin-assisted or dipped LbL, respectively. The NR also demonstrated that chemical cross-linking increases chain interdiffusion, which was more enhanced by the higher molecular weight of the PVPON binder. The spin-assisted multilayer hydrogel maintains persistent layering upon hydration but exhibits differential swelling due to alternating strata of lesser and greater cross-link densities, as templated by the initial hydrogen-bonded multilayer.

MECHANICAL PROPERTIES

Planar Multilayer Hydrogel Coatings. Because of the nanothin dimension, the mechanical properties of the LbL coating are typically characterized using AFM, which involves indenting the film with a sharp or colloidal probe and generating a force-deformation curve, which represents the elasticity of the sample. The elastic moduli of dry spin-assisted multilayer films have been reported to be in the range of 0.77−6 GPa, depending on the film composition and preparation conditions.[102,103] Because of water's plasticizing impact, the hydration of the multilayer films reduces Young's modulus by an order of magnitude, decreasing to as low as a few kPa depending on the degree of hydration.[104−107] We combined the mechanical mapping of the PMAA multilayer hydrogel with the characterization of its mechanical properties.[39] The obtained Young's modulus maps allow tracking local variations and inhomogeneities in the mechanical properties of the hydrogel across a micrometer area. The average Young's moduli of dry hydrogen-bonded $(PMAA/PVPON)_{60}$ and $(PMAA)_{60}$ multilayer hydrogel coatings using a sharp tip were ∼1.9 ± 0.2 GPa with homogeneous values throughout a 1 μm^2 area.[39] Following the general trend, ∼25- and 136-fold decreases in the $(PMAA)_{60}$ hydrogel elasticity were seen upon hydrogel hydration at pH 5 and 6.5, respectively, as measured with a colloidal probe. Specifically, Young's modulus of $(PMAA)_{60}$ was 77 ± 13 MPa at a hydration of 70 ± 2% at pH 5 and 14 ± 3 MPa at 77 ± 3% hydration at pH 6.5, indicating that the PMAA multilayer hydrogel exhibits a drastic decrease in rigidity even after a slight increase in hydration.[39] To improve the mechanical properties, one can modify the hydrogel's composition and increase its physical dimensions (thickness) and cross-link density.[108] Introducing an additional interaction between the polymer's functional groups and Zr(IV) ionic species led to a suppressed swelling and a subsequent increase in Young's modulus of the

https://doi.org/10.1021/acs.langmuir.2c00630
Langmuir XXXX, XXX, XXX−XXX

ion-containing network.[39] While the elastic modulus for both dry $(PMAA)_{60}$ and $(PMAA)_{60}$-Zr(IV) hydrogels was 2.2 ± 0.2 GPa, Zr(IV) ion loading resulted in 6- and 23-fold increases in Young's modulus for these hydrogels hydrated at pH 5 and 6.5, respectively.[39] The coordination links between the hydrogel and Zr(IV) were temporal and could be removed with an EDTA chelator, restoring the original hydrogel rigidity.[39]

Mechanical Deformations in Nonspherical Multilayer Hydrogel Capsules. Understanding the deformation of nonspherical hydrogel capsules in solution under different acidity conditions and their shape recovery is essential for advancing soft colloid materials.[39] The control of capsule deformation and the shape recovery time is vital for controlling the responses from the biological systems upon interaction with the hydrogel colloids. The mechanical stability of nonspherical capsules has been rarely explored, with a few examples of rigid ionically paired[109] and hydrogen-bonded[110] polyelectrolyte multilayer capsules.

The type and density of bonds between the polymer chains in the hydrogel can affect the shape recovery of the hydrogel capsule after stress removal. Generally, a covalently linked network can manifest elastic behavior, while the secondary bonds (e.g., hydrogen bonds or ionic pairs) lead to viscoelastic hydrogel behavior. The persistence of the cross-links tightly holding the polymeric chains in the former confers a rubber-like behavior to the hydrogel, and breaking and reforming the links in the latter should dissipate energy and relax the structure.

We showed that the cubical $(PMAA)_{13}$ hydrogel capsule's pH-induced swelling led to partial shape reversibility due to both covalent and ionic links in the network.[74] Conversely, the swelling-induced discoidal-to-ellipsoidal shape transformations of $(PMAA)_{15}$ hydrogel capsules with only covalent links in the network showed complete shape recovery.[72] In addition, we found that the stiffness of the hydrogel capsule shell is essential in capsule shape recovery.[43] We showed that volume changes from small to large cubical capsules of a more rigid $(PMAA\text{-}PVPON)_5$ hydrogel were completely reversible, and the more rigid hydrogel could better withstand the stresses of pH-triggered swelling. Conversely, the softer $(PMAA)_{20}$ single-component cubical capsule was subject to outward bending of its side faces, and the changes were only partially reversible.[43]

Cubical Capsule Shape Recovery after Large Osmotic Deformations. The deformation behavior of 5 μm cubical hydrogel microcapsules with a capsule wall made of a 10-layer (PMAA) hydrogel obtained via the templated assembly of PVPON and amine-containing PMAA copolymer (PMAA-NH_2) was studied in bulk solution at low and basic pH (Figure 11a–f). The cross-link density of at least 16 monomer units between two cross-links was necessary to obtain the hollow $(PMAA)_{10}$ capsules that could retain the cubical template shape after template dissolution (Figure 11g,h).[73] For osmotically induced deformation, the capsules were exposed to varying concentrations of a macromolecule, poly(styrenesulfonate sodium salt) (PSS; M_w = 70 kDa), that could not permeate the capsule shell, and the capsule deformations in response to the osmotic pressure differences were observed using optical fluorescence microscopy.

At pH 8 and low osmotic pressures of 6–20 kN m^{-2} induced by low concentrations (0.1–0.3 wt %) of PSS, the capsules buckled inward alongside the cubical faces (Figure 12a,b). At higher osmotic pressures (>33 kN m^{-2}), the cubical multilayer hydrogel capsules completely deformed through the inward buckling of the cubical faces and edges (Figure 12c–g).

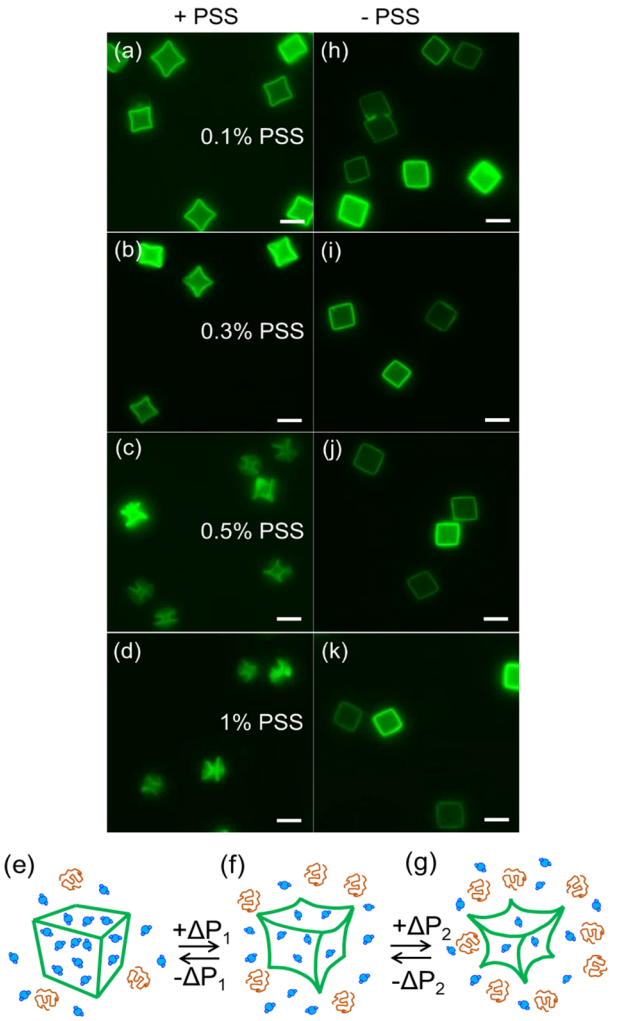

Figure 12. Optical fluorescence images of cubical $(PMAA)_{10}$ hydrogel capsules at pH 8 in the presence of PSS of (a) 0.1, (b) 0.3, (c) 0.5, and (d) 1 wt % and (h–k) after PSS was washed off with buffer at pH 8. The scale bar is 10 μm in all images. (e) The schematics show reversible deformations of the cubical PMAA capsule in response to osmotic pressure differences (f) ΔP_1 and (g) ΔP_2 at pH 8, where $\Delta P_2 > \Delta P_1$. Reproduced with permission from ref 73. Copyright 2021 American Chemical Society.

Remarkably, the removal of PSS from the capsule solution completely restored the initial cubical shape of the hydrogel capsules immediately after stress release (Figure 12h–k). The elasticity of the hydrogel capsule wall was obtained from the thin square film bulging method to be ~56 MPa, like that for elastomeric networks.[73]

In contrast, almost 3 days were necessary for these cubical hydrogel capsules to release the osmotically induced deformations after PSS removal at pH 3.[73] The different response to the osmotically induced stresses was attributed to the PSS adsorption on the capsule shell at low pH, which could be removed by the consequent exposure of the deformed cubical $(PMAA)_{10}$ capsules to pH 8. The resulting immediate swelling of the thin hydrogel restored the initial shape and size of the cubical capsule. These findings demonstrated that, unlike spherical capsules that nonuniformly buckled in response to the increased osmotic pressure by PSS, the cubical capsules showed a uniform response through the cubical face's inward buckling. These uniform inward deformations of the whole

https://doi.org/10.1021/acs.langmuir.2c00630
Langmuir XXXX, XXX, XXX–XXX

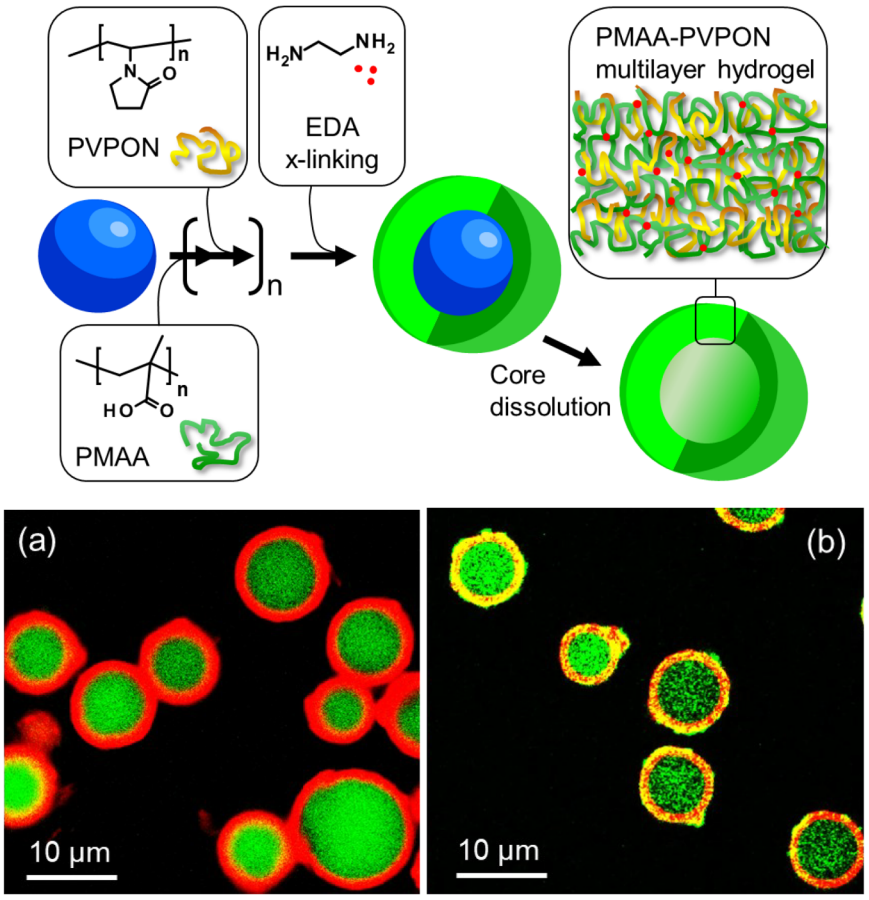

Figure 13. Schematics show the LbL assembly of PMAA (150 000 g mol^{-1}) and PVPON (1 300 000 g mol^{-1}) on sacrificial inorganic microparticles, followed by PMAA cross-linking with ethylenediamine (EDA) and template dissolution to produce $(PMAA\text{-}PVPON)_n$ interpenetrating multilayer hydrogel capsules with PVPON physically entrapped within the hydrogel. (Subscript *n* denotes the number of PMAA/PVPON bilayers.) (a) Confocal microscopy images of DOX (the red fluorescence) encapsulated in the shell of $(PMAA/PVPON)_{14}$ hydrogel capsules with the capsule cavities loaded with 4000 g mol^{-1} FITC-dextran (the green fluorescence) at (a) pH 7.5 and (b) pH 5.5. Reproduced with permission from ref 127. Copyright 2018 American Chemical Society.

capsule population in solution were attributed to the cubical shape's preset rigidity elements, including vertices and edges. These capsules are the first example of nonspherical ultrathin shells with 86 nm dry thickness that can quickly and fully restore their complex shape after its complete collapse in solution.

APPLICATIONS OF TWO-DIMENSIONAL AND THREE-DIMENSIONAL MULTILAYER HYDROGELS

Hydrogel Films for Sensing and Topical Delivery. Bulk gels and polymer networks generally demonstrate a slow diffusion-based response (from minutes to hours) and inhomogeneous swelling due to variations in the cross-link density.[1] Using ultrathin hydrogels nanostructured through controlled layering and chain interdiffusion can significantly improve the overall response time to less than seconds, overcoming one of the main barriers to rapidly responsive systems, diffusion.[33] Ultrathin multilayer hydrogels increase solvent diffusion drastically through highly stratified layering and alternating free volumes.[37,46,74] The ultrathin multilayer hydrogels have the largest swelling factor between swollen and collapsed states in response to a very narrow pH transition.[37,49] In contrast to bulk hydrogels, the layered nanothin structure allows for the integration of functional molecules at a certain depth, and these structures are not limited to a substrate shape, morphology, or size.[38,97,111] These features are essential for developing rapid-response sensors and multifunctional materials with unconventional response triggers for biomedicine.[73,81,112,113]

The potential applications of stimuli-responsive hydrogels that can vary their volume in response to guest molecules have attracted interest because of their potential as sensing systems.[114−117] The ability to detect amino acids using hydrogels is particularly intriguing because amino acids are essential building blocks for peptides, neurotransmitters, and proteins in biological organisms.[118−120] Because amino acids possess both carboxyl and amino groups, they can form strong metal complexes and can be used as excellent chelators.[121−124] We utilized the ability of $(PMAA)_n$ multilayer hydrogels to load Cu^{2+} ions to explore the stability of the $[(PMAA)_n\text{-}Cu^{2+}]$ complex in the presence of arginine, histidine, serine, glutamine, and threonine.[125] After Cu^{2+} loading, the network experienced suppressed swelling at pH >5 because of a strong interaction between the ions and the carboxylic groups of the PMAA, leading to suppressed PMAA ionization. The hydrogel swelling was recovered to some degree in the presence of histidine, serine, glutamine, and threonine because of the ion removal by these amino acids. However, arginine did not affect the hydrogel's swelling because of the high stability of the ternary PMAA-Cu^{2+}-arginine complex. The complete removal of Cu^{2+}

https://doi.org/10.1021/acs.langmuir.2c00630
Langmuir XXXX, XXX, XXX−XXX

at acidic pH demonstrated the hydrogel potential for actuation and sensing applications. This hydrogel holds considerable promise for amino acid sensing considering several unique features, including (a) easily controlled thickness at the nanoscale, (b) a high swelling capacity, (c) fast Cu^{2+} loading without chelating agents, (d) recognition of several types of amino acids, and (e) multiple detection cycles without altering the original hydrogel swelling profile.

The ability of multilayer hydrogels to change their volume in response to temperature variations might be useful in controlled delivery. For example, we showed that a thermoresponsive hydrogel $(\nu PVCL)_{30}$ consisting of a multilayer of core−shell nanogels could be utilized for topical drug delivery.[126] A nonsteroidal anti-inflammatory drug, sodium diclofenac, which is frequently given transdermally for osteoarthritis pain therapy, was loaded into the $(\nu PVCL)_{30}$ hydrogel to be released at a temperature greater than the LCST of PVCL. The free volume provided by the νPVCL nanoparticles cross-linked into the network allowed us to increase the drug-loaded amount up to 120 $\mu g/cm^2$. The hydrogel showed the sustained permeation of diclofenac through a trans-well diffusion cell used as an artificial skin membrane for up to 24 h at 32 °C, which is the typical temperature of human skin. In contrast, νPVCL nanoparticles in solution had 12 times lower diclofenac transport than that for the νPVCL hydrogel, indicating a much higher contact area of the hydrogel than that of nanogels distributed in solution.

Another unique feature of this multilayer νPVCL hydrogel is its ability to incorporate multiple drugs loaded into the nanogels before the LbL assembly and cross-linking into a hydrogel matrix. Thus, three fluorescent dyes, including Nile red, fluorescein, and DAPI, were stacked in a multilayer network as 12-layer bottom, middle, and top strata, respectively, indicating the potential use of the hybrid hydrogel as a multidrug delivery system.[126]

Hollow Multilayer Hydrogel Capsules for Controlled Delivery. *Encapsulation of Small Molecules.* We developed interpenetrated multilayer hydrogel capsules via the multilayer assembly of PMAA (150 000 g mol^{-1}) and PVPON (1 300 000 g mol^{-1}) on porous and solid silica microparticles, followed by the cross-linking of the PMAA multilayers with ethylenediamine, which results in the physical entrapment of PVPON layers within the PMAA network (Figure 13).[127] Using the pH-sensitive interpenetrated hydrogel shell results in efficient control of the encapsulation of a broad spectrum of hydrophilic compounds, including those with molecular weights of less than 1000 g mol^{-1}. We studied the encapsulation of low-molecular-weight hydrophilic compounds by combining pH-induced postloading and dextran interaction with the hydrogel capsule shell. Two-component $(PMAA/PVPON)_n$ hydrogel capsules containing physically entrapped PVPON were used to postload hydrophilic small molecules, including doxorubicin (DOX) and Alexa Fluor 532 carboxylate, and FITC-dextran macromolecules with M_w from 4000 to 40 000 g mol^{-1}. The $(PMAA/PVPON)_{14}$ capsules cross-linked for either 4 or 24 h could encapsulate hydrophilic molecules with M_w starting at 4000 g mol^{-1} at pH 7.5 when the capsules were swollen. The strong interaction between high-molecular-weight dextrans and the hydrogel network of the (PMAA/PVPON) capsule was used to seal the hydrogel capsule shell, resulting in a significant reduction in the capsule permeability.

Unlike dextrans and Alexa Fluor 532 carboxylate, which were trapped in the hydrogel capsule interior cavity, DOX was trapped inside the hydrogel capsule shell because of a strong electrostatic interaction between positively charged DOX molecules and a negatively charged dextran that sealed the capsule shell (Figure 13a,b). This two-component (PMAA/PVPON) hydrogel capsule with an interpenetrated (PMAA/PVPON) shell can be a versatile platform for delivering a broad spectrum of hydrophilic molecules, including the codelivery of multiple compounds.

Encapsulation and Release of Therapeutic Nucleic Acids. The encapsulation and delivery of nucleic can be a viable treatment for inherited or acquired disorders.[128,129] The interpenetrated $(PMAA/PVPON)_n$ multilayer hydrogel capsules assembled on porous $CaCO_3$ sacrificial templates and cross-linked with an enzyme-degradable cross-linker were demonstrated to encapsulate double-stranded DNA and G-quadruplex oligonucleotides within the hydrogel capsule interior.[130] The $(PMAA/PVPON)_6$ capsules carrying G-quadruplex DNA released 50% of the encapsulated G-quadruplex DNA after 2 h of exposure to glutathione.

The multilayer hydrogel shell of the $(PMAA/PVPON)_6$ capsules was also susceptible to mechanical destruction by ultrasound.[130] The G-quadruplex DNA-loaded $(PMAA/PVPON)_6$ hydrogel capsules with 37 amol of G-quadruplex oligonucleotides per capsule were destroyed by ultrasound irradiation. Significantly, neither encapsulation nor release from the $(PMAA/PVPON)_{13}$ hydrogel capsules via degradation or ultrasound affected the secondary structure of G-quadruplex DNA. The capsule demonstrated a 2000-fold increase in the amount of encapsulated DNA by utilizing the entire volume of the hydrogel capsule for DNA encapsulation and a more rigid (PMAA/PVPON) interpenetrated multilayer hydrogel shell.

Interaction of Nonspherical Multilayer Hydrogel Capsules with Cells. We found the effect of the hydrogel capsule shape on the interaction with immune cells, breast cancer cells, and endothelial cells.[72] The discoidal hydrogel capsules combined the critical characteristics of the erythrocyte cells, including the discoidal shape, hollow structure, and low rigidity with the reversible pH-responsiveness of PMAA in a carrier where chemical stimuli can trigger the release in the tumor lesion where the extracellular pH is acidic (pH 6.5−5.0), unlike that in normal tissue (pH 7.2−7.4).

In contrast to the solid cores, a lesser cellular association/internalization of soft hydrogel capsules was seen with HMVEC endothelial and 4T1 breast cancer cells.[72] Also, a 7.6-fold decrease in the particle-to-macrophage association was provided by the PMAA discoidal hydrogel capsules compared to the solid particles as a result of the low rigidity of the PMAA hydrogel capsules. The cell interaction of the discoidal capsules was persistently 60% lower than that for the spherical capsules. Thus, the cellular internalization by 4T1 breast cancer cells was 5-fold smaller for the discoidal hydrogel capsules compared to that of the spherical ones, indicating the potential for prolonged circulation of the discoidal hydrogel capsules.

Nonhollow Multilayer Hydrogel Particles. *Effect of Shape on Cell Interaction.* The effect of the shape of nonhollow multilayer hydrogel particles was studied using human cervical carcinoma HeLa cells.[76] The cubical and spherical (PMAA) multilayer hydrogel particles with disulfide links were obtained by cross-linking PMAA with cystamine within hydrogen-bonded multilayers of (PMAA/PVPON) on sacrificial mesoporous templates. The accumulation of positive charge within the cystamine-cross-linked PMAA hydrogel particles at pH <5 could facilitate their endosomal/lysosomal escape via inducing endosomal disruption because of the hydrogel swelling.[76]

https://doi.org/10.1021/acs.langmuir.2c00630
Langmuir XXXX, XXX, XXX−XXX

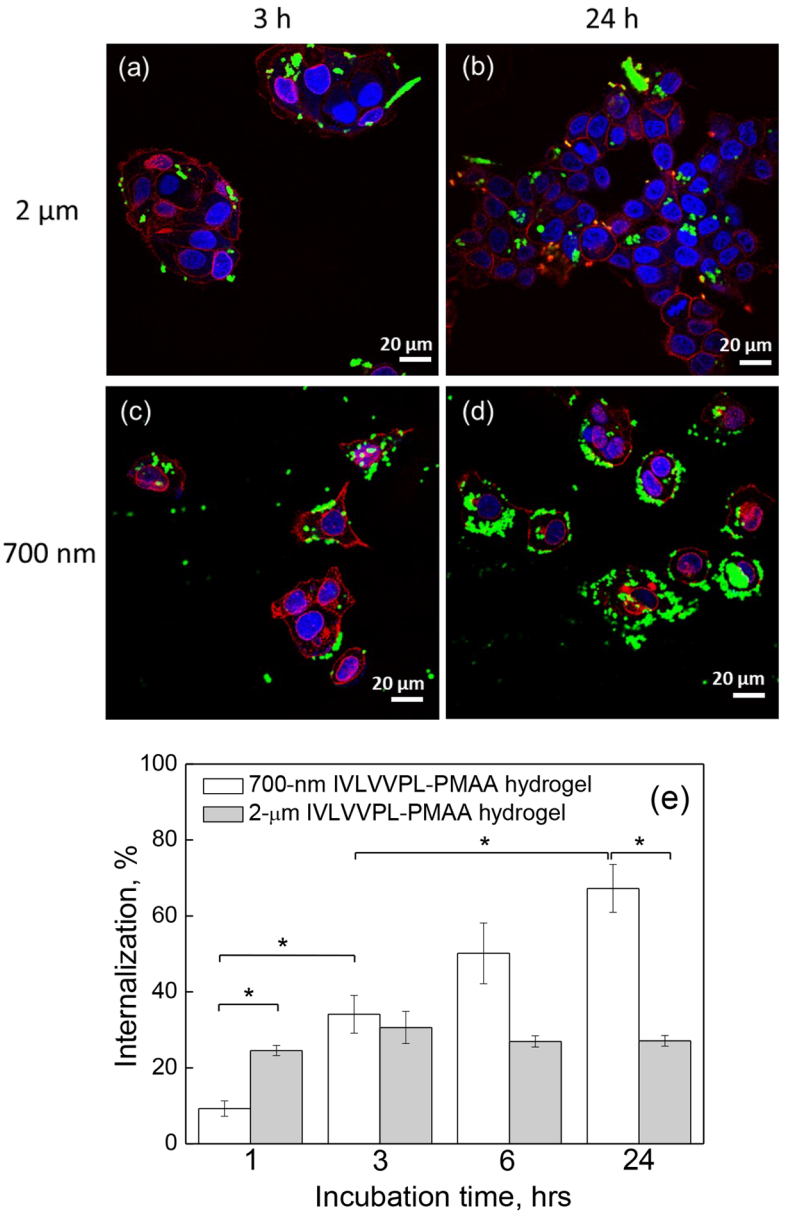

Figure 14. (a–d) Confocal microscopy images of MCF-7 cells after incubation with IPLVVPL-PMAA hydrogel cubes of 2 μm and 700 nm for 3 or 24 h. The cell nuclei and membranes are stained with DAPI (blue) and wheat germ agglutinin and with Alexa Fluor 555 conjugate (WGA Alexa 555) (red), respectively. The hydrogel cubes have green fluorescence. The scale bar is 20 μm in all images. (e) Internalization (%) of 2 μm and 700 nm IPLVVPL-PMAA hydrogel cubes by MCF-7 cell (*$p < 0.05$). Reproduced with permission from ref 78. Copyright 2018 American Chemical Society.

The spherical and cubical PMAA hydrogel particles retained their respective 3D shapes in the dry state, and the corresponding hydrogel capsules collapsed upon drying. The ability of the multilayer hydrogel particles to preserve their 3D structure indicates that both PMAA and PVPON polymers can infiltrate the pores of the porous template during the deposition process and that the (PMAA/PVPON) multilayers can be formed inside pores.

The cystamine-cross-linked PMAA hydrogel particles had a swelling profile similar to that of nondegradable ethylenediamine-linked hydrogel particles. However, the overall swelling ratios were smaller than those of the EDA-cross-linked cubes or spheres.[75,76] The lower 1.5–1.2-fold swelling ratios of the $(PMAA)_5$ biodegradable hydrogels were due to their more hydrophobic interior because of the hydrophobic cross-linker, cystamine.

The cell internalization and viability in the presence of the DOX-loaded cubical and spherical particles indicated that once the particles were taken up by the HeLa cells, DOX was rapidly released to enter the cell nuclei and kill the cells.[76] Because the amounts of DOX per particle in the cubical and spherical hydrogels were similar, the 12% higher cell cytotoxicity observed for the $(PMAA)_5$ hydrogel spheres as compared to that of the cubes within the first 10 h of incubation reflected the effect of the hydrogel particle shape on cellular internalization. Because of a higher wrapping energy barrier for cubes than for spheres, spheres can be internalized faster.[76] Indeed, our results on 12% higher cell cytotoxicity observed for the $(PMAA)_5$ hydrogel spheres within the 10 h incubation indicate that the membrane adhesion process is critical in the initial steps of cell internalization. However, the similar cytotoxicity of DOX-loaded $(PMAA)_5$ spheres and cubes after 24 and 48 h of

https://doi.org/10.1021/acs.langmuir.2c00630
Langmuir XXXX, XXX, XXX–XXX

incubation indicated similar internalization of the hydrogel cubes at longer times.[76]

Delivery of Anticancer Therapeutics to Cells. The hydrophobic interior of the PMAA hydrogel cubes cross-linked with cystamine allowed for the encapsulation of 7-(benzylamino)-3,4-dihydro-pyrrolo[4,3,2-de]quinolin-8(1*H*)-one (BA-TPQ), a hydrophobic anticancer drug with high potency, and its delivery to p53 mutant cancer cell lines.[77] The BA-TPQ-loaded cubical PMAA hydrogel microparticles completely disintegrated after 3 h at 5 mM GSH and released BA-TPQ into the cancer cells. The BA-TPQ-loaded PMAA cubes had a 2-fold higher permeability than nonencapsulated BA-TPQ through the Caco-2 cell monolayer used as a model for oral delivery because of the bioadhesiveness of PMAA. Although not cytotoxic to normal liver cells (CL48 and LO2 hepatocytes), the BA-TPQ-hydrogel cubes reduced the viability of HepG2 and Huh7 liver cancer cells by 40% compared to the nonencapsulated drug. These results, combined with lower IC_{50} values for BA-TPQ-loaded PMAA hydrogel cubes, demonstrated a significantly improved BA-TPQ ability to suppress the expression of oncoproteins in liver cancer cells, which can be a promising approach for clinical liver cancer chemotherapy.

Effect of Size and Targeting on the Interaction with Cancer Cells. We developed a hepsin-targeting modification of the PMAA hydrogel cubes using the Ile-Pro-Leu-Val-Val-Pro-Leu peptide (IPLVVPL) to promote specific tumor targeting.[78] Specifically, the IPLVVPL peptide was conjugated to the hydrogel network in a thiol-amine reaction utilizing remaining free amine groups from PMAA cross-linked with cystamine and the sulfhydryl groups of the IPLVVPL-PEG-Cyc-Lys[FITC] peptide. The 700 nm and 2 μm IPLVVPL-PMAA hydrogel cubes contained the same quantity of the conjugated peptide and had the same surface charge. Notably, the peptide conjugation did not affect the hydrogel cubes' 3D shape, size, and DOX loading or release but reduced GSH diffusion inside the particles, prolonging IPLVVPL-PMAA hydrogel degradation in the presence of intracellular amounts of GSH. Conversely, the disintegration of the hydrogel in the presence of intracellular amounts of GSH considerably boosted the DOX release from the IPLVVPL-PMAA hydrogel cubes from 58 ± 4 to 97 ± 1%.[78]

The 700 nm and 2-μm peptide-free PMAA hydrogel cubes demonstrated different internalization kinetics by hepsin-positive MCF-7 cells.[78] Although the cellular uptake of 700 nm hydrogel cubes increased consistently from 3.8 ± 0.9 to 34 ± 6% after 1 and 24 h of incubation, respectively, the 2-fold increase in cellular uptake was achieved for 2 μm cubes at between 1 and 3 h of incubation. The enhanced cellular uptake of 2 μm peptide-free hydrogel cubes was due to the sedimentation acceleration and cell-binding augmentation generated by the larger particle size compared to those of smaller 700 nm PMAA hydrogels.

In contrast, the cell-specific uptake of 2 μm IPLVVPL-PMAA particles was 2.5-fold lower than that of the 700 nm hydrogel cubes after 24 h of incubation (Figure 14). The internalization of 700 nm IPLVVPL-PMAA hydrogels was also 2-fold greater than that of the 700 nm peptide-free PMAA hydrogel cubes at each time point because of the strong affinity of the IPLVVPL peptide to hepsin-positive MCF-7 cells.

Finally, the cellular uptake of the 700 nm peptide-modified PMAA hydrogel cubes was also cell-specific. Thus, the hepsin-positive MCF-7 and SK-OV-3 cells took up the IPLVVPL-PMAA hydrogels at a 3- to 10-fold faster rate than did the hepsin-negative PC-3 cells.[78] Thus, these PMAA multilayer cubical hydrogel particles have a strong potential as active and passive targeting drug delivery carriers because of their negative surface charge, soft hydrogel morphology, ease of ligand conjugation, and size tunability.

CONCLUSIONS AND OUTLOOK

Nature's complex hierarchical structures are manifested in diverse and well-regulated mechanical and biological behaviors desirable for current industrial and biomedical applications. Layered hydrogel approaches have been indicated as being capable of mimicking natural layered materials' properties, including nanostructured morphology, significant and reversible stimuli-triggered changes, and controlled rigidities. Stimuli-responsive hydrogels based on the multilayer assembly of polymers have opened new opportunities in the design of hierarchically organized networks. The multilayer hydrogel assembly using the layer-by-layer adsorption of polymers at surfaces can be realized on numerous geometries, including planar and 3D surfaces of spherical and anisotropic shapes, and produce ionic, both anionic and cationic, and nonionic multilayer hydrogel coatings with a nanoscale thickness (<100 nm). This Feature Article provides an overview of primary studies from our laboratory on nanothin multilayer hydrogel films, bringing about fundamental knowledge on the synthesis of surface-anchored and free-standing pH- and temperature-responsive films. The effect of assembly strategies on hydrogels' internal architectures and their solution behavior is discussed. This Feature Article also covers significant advances in multilayer hydrogel colloids, including anisotropic hollow capsules and nonhollow hierarchically structured microparticles, and summarizes studies on particle mechanical properties in solutions in response to environmental stimuli. The non-spherical thin multilayer hydrogel shells are attractive for their potential to mimick cellular membrane behavior and bring about an understanding of cell biological functions, including cell performance in the flow.

Along with vital fundamental knowledge, these findings present new challenges and raise questions about opportunities for the synthesis and applications of nanothin hydrogel materials with complex hierarchical architecture that need to be further explored. Knowing the structural organization of the multilayer hydrogel coatings will extend the rational design of hydrogel-based materials with predictable and well-tunable properties, broadening their practical applications. For example, understanding the fundamental relationships among multilayer hydrogel architectures, chemical compositions, and assembly strategies will help to design stimuli-responsive complex multistack systems which would break through the traditional bulk hydrogels with uniform architectures. This knowledge will compose the experimental basis for developing nonconventional hydrogel-based materials with highly controlled properties, contributing to modern polymer science. The multistack multilayer hydrogels can be used to produce multidepot hydrogels for the selective loading/diffusion of functional molecules or the confined incorporation of optical markers for drug delivery or sensing applications, respectively. The synthesis and the effects on the properties of nanothin multilayer hydrogel coatings using other LbL approaches, for example, spray- versus spin-assisted LbL, need to be addressed to uncover new possibilities to control structural and functional properties of the multilayer hydrogel coatings. Data analysis tools that allow quantitative parameter retrieval in the systems changing the

https://doi.org/10.1021/acs.langmuir.2c00630
Langmuir XXXX, XXX, XXX−XXX

composition and internal structure because of physical/chemical modifications need to be further developed to advance the knowledge on the effects of the architectural hierarchy of multilayer hydrogel coatings. Finally, the design and synthesis of nonspherical multilayer hydrogel colloids with controlled shape changes in response to environmental stimuli would increase our understanding of various biological responses and create hydrogel structures with precisely tuned environmental responses. Related to that, expanding the spectrum of environmental stimuli for multilayer hydrogel coatings and colloids, including light, magnetic fields, and ultrasound, will be essential for further developing the field of responsive networks.

AUTHOR INFORMATION

Corresponding Author

Eugenia Kharlampieva − *Department of Chemistry, Center for Biomaterials and Biointegration, and O'Neal Comprehensive Cancer Center, The University of Alabama at Birmingham, Birmingham, Alabama 35294, United States;* orcid.org/0000-0003-0227-0920

Authors

Veronika Kozlovskaya − *Department of Chemistry, The University of Alabama at Birmingham, Birmingham, Alabama 35294, United States;* orcid.org/0000-0001-9089-4842

Maksim Dolmat − *Department of Chemistry, The University of Alabama at Birmingham, Birmingham, Alabama 35294, United States;* orcid.org/0000-0002-4918-7342

Complete contact information is available at: https://pubs.acs.org/10.1021/acs.langmuir.2c00630

Notes

The authors declare no competing financial interest.

Biographies

Veronika Kozlovskaya received her Ph.D. in polymer chemistry at the Stevens Institute of Technology in 2008 and was a postdoctoral fellow at the Georgia Institute of Technology. She joined the Kharlampieva research group at the University of Alabama at Birmingham in 2010. Dr. Kozlovskaya's research interests include the design and synthesis of responsive hydrogels and polymeric containers for drug delivery, macromolecular self-assembly, surface modification, and biomaterial characterization at the nanoscale.

Maksim Dolmat received his B.S. in chemistry from Belarusian State University in 2016. He is currently a Ph.D. student at the University of Alabama at Birmingham in Professor Kharlampieva's laboratory. His research focuses on the layer-by-layer assembly of thin stimuli-responsive hydrogels, including coatings and shaped particles for sensing and controlled delivery. He is particularly interested in tuning hydrogel mechanical properties by controlling their architecture using neutron reflectometry and atomic force microscopy.

Eugenia Kharlampieva is a distinguished professor in the Department of Chemistry at the University of Alabama at Birmingham (UAB) and a College of Arts and Sciences Endowed Faculty Scholar. She also serves as an associate director of the UAB Center for Nanoscale Materials and Biointegration. She received her Ph.D. in polymer science from the Stevens Institute of Technology and postdoctoral training in materials science and engineering at the Georgia Institute of Technology. Her research centers on the intersection of polymer chemistry, nanotechnology, and biomedical science to develop polymer materials for therapeutic, sensing, and environmental applications. Dr. Kharlampieva received the NSF CAREER Award, the UAB Dean's Award for Excellence in Mentorship, the UAB Interdisciplinary Innovation Award, and the Faculty Innovator Entrepreneurship Award.

ACKNOWLEDGMENTS

This work was supported by NSF DMR award no. 1904816.

REFERENCES

(1) Danielsen, S.; Beech, H.; Wang, S.; El-Zaatari, B.; Wang, X.; Sapir, L.; Ouchi, T.; Wang, Z.; Johnson, P.; Hu, Y.; Lundberg, D. J.; Stoychev, G.; Craig, S. L.; Johnson, J. A.; Kalow, J. A.; Olsen, B. D.; Rubinstein, M. Molecular Characterization of Polymer Networks. *Chem. Rev.* **2021**, *121*, 5042−5092.

(2) Zhu, Y.; Haghniaz, R.; Hartel, M. C.; Mou, L.; Tian, X.; Garrido, P. R.; Wu, Z.; Hao, T.; Guan, S.; Ahadian, S.; Kim, H.-J.; Jucaud, V.; Dokmeci, M. R.; Khademhosseini, A. Recent Advances in Bioinspired

https://doi.org/10.1021/acs.langmuir.2c00630
Langmuir XXXX, XXX, XXX−XXX

Hydrogels: Materials, Devices, and Biosignal Computing, *ACS Biomater. Sci. Eng.* **2021**, DOI: 10.1021/acsbiomaterials.1c00741.
(3) Li, Y.; Yang, H. Y.; Lee, D. S. Advances in biodegradable and injectable hydrogels for biomedical applications. *J. Controlled Release* **2021**, *330*, 151−160.
(4) Correa, S.; Grosskopf, A. K.; Hernandez, H. L.; Chan, D.; Yu, A. C.; Stapleton, L. M.; Appel, E. A. Translational Applications of Hydrogels. *Chem. Rev.* **2021**, *121*, 11385−11457.
(5) Means, A. K.; Shrode, C. S.; Whitney, L. V.; Ehrhardt, D. A.; Grunlan, M. A. Double Network Hydrogels that Mimic the Modulus, Strength, and Lubricity of Cartilage. *Biomacromolecules* **2019**, *20*, 2034−2042.
(6) Vashahi, F.; Martinez, M. R.; Dashtimoghadam, E.; Fahimipour, F.; Keith, A. M.; Bersenev, E. A.; Ivanov, D. A.; Zhulina, E. B.; Popryadukhin, P.; Matyjaszewski, K.; Vatankhah-Varnosfaderani, M.; Sheiko, S. S. Injectable bottlebrush hydrogels with tissue-mimetic mechanical properties. *Sci. Adv.* **2022**, *8*, eabm2469.
(7) Tayler, I. M.; Stowers, R. S. Engineering hydrogels for personalized disease modeling and regenerative medicine. *Acta Biomater.* **2021**, *132*, 4−22.
(8) Shih, H.; Fraser, A. K.; Lin, C.-C. Interfacial Thiol-Ene Photoclick reactions for forming multilayer hydrogels. *ACS Appl. Mater. Interfaces* **2013**, *5*, 1673−1680.
(9) Chen, J.; Peng, Q.; Peng, X.; Han, L.; Wang, X.; Wang, J.; Zeng, H. Recent Advances in Mechano-responsive hydrogels for biomedical applications. *ACS Appl. Polym. Mater.* **2020**, *2*, 1092−1107.
(10) He, X.; Wang, S.; Zhou, J.; Zhang, D.; Xue, Y.; Yang, X.; Che, L.; Li, D.; Xiao, S.; Liu, S.; Zheng, S. Y.; Yang, J. Versatile and Simple Strategy for Preparing Bilayer Hydrogels with Janus Characteristics. *ACS Appl. Mater.Interfaces* **2022**, *14*, 4579−4587.
(11) Vázquez-González, M.; Willner, I. Stimuli-Responsive Biomolecule-Based Hydrogels and Their Applications. *Angew. Chem., Int. Ed. Engl.* **2020**, *59*, 15342−15377.
(12) Kozlovskaya, V.; Kharlampieva, E. Self-Assemblies of Thermoresponsive Poly(N-vinylcaprolactam) Polymers for Applications in Biomedical Field. *ACS Applied Polym. Mater.* **2020**, *2*, 26−39.
(13) Means, A. K.; Ehrhardt, D. A.; Whitney, L. V.; Grunlan, M. A. Thermoresponsive Double Network Hydrogels with Exceptional Compressive Mechanical Properties. *Macromol. Rapid Commun.* **2017**, *38*, 1700351.
(14) Khutoryanskaya, O. V.; Mayeva, Z. A.; Mun, G. A.; Khutoryanskiy, V. V. Designing Temperature-Responsive Biocompatible Copolymers and Hydrogels Based on 2-Hydroxyethyl(meth)acrylates. *Biomacromolecules* **2008**, *9*, 3353−3361.
(15) Longo, G. S.; Olvera de la Cruz, M.; Szleifer, I. Molecular Theory of Weak Polyelectrolyte Gels: The Role of pH and Salt Concentration. *Macromolecules* **2011**, *44*, 147−158.
(16) Flory, P. J.; Rehner, J. J. Statistical mechanics of cross-linked polymer networks. II Swelling. *J. Chem. Phys.* **1943**, *11*, 521−526.
(17) Longo, G. S.; Olvera de la Cruz, M.; Szleifer, I. Molecular theory of weak polyelectrolyte thin films. *Soft Matter* **2012**, *8*, 1344−1354.
(18) Bittner, S. M.; Pearce, H. A.; Hogan, K. J.; Smoak, M. M.; Guo, J. L.; Melchiorri, A. J.; Scott, D. W.; Mikos, A. G. Swelling Behaviors of 3D Printed Hydrogel and Hydrogel-Microcarrier Composite Scaffolds. *Tissue Eng. Part A* **2021**, *27*, 665−678.
(19) Matsumoto, A.; Kurata, T.; Shiino, D.; Kataoka, K. Swelling and Shrinking Kinetics of Totally Synthetic, Glucose-Responsive Polymer Gel Bearing Phenylborate Derivative as a Glucose-Sensing Moiety. *Macromolecules* **2004**, *37*, 1502−1510.
(20) Zhang, X.-Z.; Xu, X.-D.; Cheng, S.-X.; Zhuo, R.-X. Strategies to improve the response rate of thermosensitive PNIPAAm hydrogels. *Soft Matter* **2008**, *4*, 385−391.
(21) Zhang, X.; Guan, Y.; Zhang, Y. Ultrathin Hydrogel Films for Rapid Optical Biosensing. *Biomacromolecules* **2012**, *13*, 92−97.
(22) Tanaka, T.; Fillmore, D. J. Kinetics of swelling of gels. *J. Chem. Phys.* **1979**, *70*, 1214−1218.
(23) Tokarev, I.; Minko, S. Stimuli-responsive hydrogel thin films. *Soft Matter* **2009**, *5*, 511−524.
(24) Marcombe, R.; Cai, S.; Hong, W.; Zhao, X.; Lapusta, Y.; Suo, Z. A theory of constrained swelling of a pH-sensitive hydrogel. *Soft Matter* **2010**, *6*, 784−793.
(25) Toomey, R.; Freidank, D.; Rühe, J. Swelling behavior of thin, surface-attached polymer networks. *Macromolecules* **2004**, *37*, 882−887.
(26) Strachota, B.; Oleksyuk, K.; Strachota, A.; Šlouf, M. Porous hybrid poly(N-isopropylacrylamide) hydrogels with very fast volume response to temperature and pH. *Eur. Polym. J.* **2019**, *120*, 109213.
(27) Franke, D.; Gerlach, G. Studies on porosity in poly(N-isopropylacrylamide) hydrogels for fast-responsive piezoresistive microsensors. *J. Sens. Sens. Syst.* **2021**, *10*, 93−100.
(28) Kuroki, H.; Islam, C.; Tokarev, I.; Hu, H.; Liu, G.; Minko, S. Tunable Ultrathin Membranes with Nonvolatile Pore Shape Memory. *ACS Appl. Mater. Interfaces* **2015**, *7*, 10401−10406.
(29) Seidi, F.; Zhao, W.-F.; Xiao, H.-N.; Jin, Y.-C.; Saeb, M. R.; Zhao, C.-S. Advanced Surfaces by Anchoring Thin Hydrogel Layers of Functional Polymers. *Chin. J. Polym. Sci.* **2021**, *39*, 14−34.
(30) Chollet, B.; Li, M.; Martwong, E.; Bresson, B.; Fretigny, C.; Tabeling, P.; Tran, Y. Multiscale Surface-Attached Hydrogel Thin Films with Tailored Architecture. *ACS Appl. Mater. Interfaces.* **2016**, *8*, 11729−11738.
(31) Kozlovskaya, V.; Kharlampieva, E.; Mansfield, M. L.; Sukhishvili, S. A. Poly(methacrylic acid) hydrogel films and capsules: Response to pH and ionic strength, and encapsulation of macromolecules. *Chem. Mater.* **2006**, *18*, 328−336.
(32) Yang, S. Y.; Rubner, M. F. Micropatterning of polymer thin films with pH-sensitive and cross-linkable hydrogen-bonded polyelectrolyte multilayers. *J. Am. Chem. Soc.* **2002**, *124*, 2100.
(33) Kozlovskaya, V.; Kharlampieva, E.; Erel, I.; Sukhishvili, S. A. Multilayer-Derived, Ultrathin, Stimuli-Responsive Hydrogels. *Soft Matter* **2009**, *5*, 4077−4087.
(34) Richardson, J. J.; Cui, J.; Björnmalm, M.; Braunger, J. A.; Ejima, H.; Caruso, F. Innovation in Layer-by-Layer Assembly. *Chem. Rev.* **2016**, *116*, 14828−14867.
(35) Nicolas, H.; Yuan, B.; Xu, J.; Zhang, X.; Schönhoff, M. pH-Responsive Host-Guest Complexation in Pillar[6]arene-Containing Polyelectrolyte Multilayer Films. *Polymers* **2017**, *9*, 719.
(36) Easley, A. D.; Shaligram, S. V.; Echols, I. J.; Nixon, K.; Regen, S. L.; Lutkenhaus, J. L. Layer-by-Layer Nanoarchitectonics of Electrochemically Active Thin Films Comprised of Radical-Containing Polymers. *J. Electrochem. Soc.* **2022**, *169*, 020510.
(37) Wang, Y.; Kozlovskaya, V.; Arcibal, I.; Cropek, D.; Kharlampieva, E. Highly swellable ultrathin poly(4-vinylpyridine) multilayer hydrogels with pH-triggered surface wettability. *Soft Matter* **2013**, *9*, 9420−9429.
(38) Kozlovskaya, V.; Chen, J.; Zavgorodnya, O.; Hasan, M. B.; Kharlampieva, E. Multilayer Hydrogel Capsules with Interpenetrated Network Shell for Encapsulation of Small Molecules. *Langmuir* **2018**, *34*, 11832−11842.
(39) Vergara, D.; Bellomo, C.; Zhang, X.; Vergaro, V.; Tinelli, A.; Lorusso, V.; Rinaldi, R.; Lvov, Y. M.; Leporatti, S.; Maffia, M. Lapatinib/Paclitaxel polyelectrolyte nanocapsules for overcoming multidrug resistance in ovarian cancer. *Nanomed.: Nanotechnol. Biol. Med.* **2012**, *8*, 891−899.
(40) Dolmat, M.; Kozlovskaya, V.; Cropek, D. M.; Kharlampieva, E. Free-standing nanothin hydrogels: Effects of composition and pH-dependent hydration on mechanical properties. *ACS Appl. Polym. Mater.* **2021**, *3*, 3960−3971.
(41) Liang, X.; Kozlovskaya, V.; Chen, Y.; Zavgorodnya, O.; Kharlampieva, E. Thermosensitive multilayer hydrogels of poly(N-vinylcaprolactam) as nanothin films and shaped capsules. *Chem. Mater.* **2012**, *24*, 3707−3719.
(42) Kozlovskaya, V.; Kharlampieva, E. Anisotropic Particles through Multilayer Assembly. *Macromol. Biosci.* **2022**, *22*, 2100328.
(43) Kozlovskaya, V.; Wang, Y.; Higgins, W.; Chen, J.; Chen, Y.; Kharlampieva, E. pH-Triggered Shape Response of Cubical Ultrathin Hydrogel Capsules. *Soft Matter* **2012**, *8*, 9828−9839.

https://doi.org/10.1021/acs.langmuir.2c00630
Langmuir XXXX, XXX, XXX−XXX

(44) Such, G. K.; Quinn, J. F.; Quinn, A.; Tjipto, E.; Caruso, F. Assembly of Ultrathin Polymer Multilayer Films by Click Chemistry. *J. Am. Chem. Soc.* **2006**, *128*, 9318−9319.
(45) She, S.; Li, Q.; Shan, B.; Tong, W.; Gao, C. Fabrication of Red-Blood-Cell-Like Polyelectrolyte Microcapsules and Their Deformation and Recovery Behavior Through a Microcapillary. *Adv. Mater.* **2013**, *25*, 5814−5818.
(46) Higgins, W.; Kozlovskaya, V.; Alford, P. A.; Ankner, J. F.; Kharlampieva, E. Stratified temperature-responsive multilayer hydrogels of poly(N-vinylpyrrolidone) and poly(N-vinylcaprolactam): Effect of hydrogel architecture on properties. *Macromolecules* **2016**, *49*, 6953−6964.
(47) Díez-Pascual, A. M.; Rahdar, A. LbL Nano-Assemblies: A Versatile Tool for Biomedical and Healthcare Applications. *Nanomaterials* **2022**, *12*, 949.
(48) Cho, J.; Char, K.; Hong, J.-D.; Lee, K.-B. Fabrication of Highly Ordered Multilayer Films Using a Spin Self-Assembly Method. *Adv. Mater.* **2001**, *13*, 1076−1078.
(49) Kozlovskaya, V.; Zavgorodnya, O.; Wang, Y.; Ankner, J. F.; Kharlampieva, E. Tailoring Architecture of Nanothin Hydrogels: Effect of layering on pH-triggered swelling. *ACS Macro Lett.* **2013**, *2*, 226−229.
(50) Zavgorodnya, O.; Kozlovskaya, V.; Liang, X.; Kothalawala, N.; Catledge, S.; Dass, A.; Kharlampieva, E. Temperature-responsive properties of nanothin poly(N-vinylcaprolactam) multilayer hydrogels in the presence of Hofmeister anions. *Mater. Res. Exp.* **2014**, *1*, 035039.
(51) Zavgorodnya, O.; Kozlovskaya, V.; Kharlampieva, E. Nanostructured highly-swollen hydrogels: Complexation with amino acids through copper (II) ions. *Polymer* **2015**, *74*, 94−107.
(52) Kozlovskaya, V.; Zavgorodnya, O.; Ankner, J. F.; Kharlampieva, E. Controlling internal organization of multilayer poly(methacrylic acid) hydrogels with polymer molecular weight. *Macromolecules* **2015**, *48*, 8585−8593.
(53) Kozlovskaya, V.; Stockmal, K.; Higgins, W.; Ankner, J. F.; Morgan, S.; Kharlampieva, E. Architecture of Hydrated Multilayer Poly(methacrylic acid) Hydrogels: Effect of Solution pH. *ACS Appl. Polym. Mater.* **2020**, *2*, 2260−2273.
(54) Zavgorodnya, O.; Carmona-Moran, C. A.; Kozlovskaya, V.; Liu, F.; Wick, T. M.; Kharlampieva, E. Temperature-Responsive Nanogel Multilayers of Poly(N-Vinylcaprolactam) for Topical Drug Delivery. *J. Colloid Interface Sci.* **2017**, *506*, 589−602.
(55) Cheng, W.; Campolongo, M.; Tan, S.; Luo, D. Freestanding Ultrathin Nano-Membranes via Self-Assembly. *Nano Today* **2009**, *4*, 482−493.
(56) Fujie, T.; Matsutani, N.; Kinoshita, M.; Okamura, Y.; Saito, A.; Takeoka, S. Adhesive, Flexible, and Robust Polysaccharide Nanosheets Integrated for Tissue-Defect Repair. *Adv. Funct. Mater.* **2009**, *19*, 2560−2568.
(57) Schuster, C.; Rodler, A.; Tscheliessnig, R.; Jungbauer, A. Freely Suspended Perforated Polymer Nanomembranes For Protein Separations. *Sci. Rep.* **2018**, *8*, 4410.
(58) Baxamusa, S.; Stadermann, M.; Aracne-Ruddle, C.; Nelson, A.; Chea, M.; Li, S.; Youngblood, K.; Suratwala, T. Enhanced Delamination of Ultrathin Free-Standing Polymer Films via Self-Limiting Surface Modification. *Langmuir* **2014**, *30*, 5126−5132.
(59) Lutkenhaus, J.; Hrabak, K.; McEnnis, K.; Hammond, P. Elastomeric Flexible Free-Standing Hydrogen-Bonded Nanoscale Assemblies. *J. Am. Chem. Soc.* **2005**, *127*, 17228−17234.
(60) Mamedov, A.; Kotov, N. Free-Standing Layer-by-Layer Assembled Films of Magnetite Nanoparticles. *Langmuir* **2000**, *16*, 5530−5533.
(61) Lavalle, P.; Boulmedais, F.; Ball, V.; Mutterer, J.; Schaaf, P.; Voegel, J. Free Standing Membranes Made of Biocompatible Polyelectrolytes Using the Layer-by-Layer Method. *J. Membr. Sci.* **2005**, *253*, 49−56.
(62) Jiang, C.; Markutsya, S.; Pikus, Y.; Tsukruk, V. Freely Suspended Nanocomposite Membranes as Highly Sensitive Sensors. *Nat. Mater.* **2004**, *3*, 721−728.
(63) Kelly, K.; Schlenoff, J. Spin-Coated Polyelectrolyte Coacervate Films. *ACS Appl. Mater. Interfaces* **2015**, *7*, 13980−13986.
(64) Zimnitsky, D.; Shevchenko, V.; Tsukruk, V. Perforated, Freely Suspended Layer-by-Layer Nanoscale Membranes. *Langmuir* **2008**, *24*, 5996−6006.
(65) Manabe, K.; Belbekhouche, S. Construction of Low-Wettable Free-Standing Layer-by-Layer Multilayer for Fibrinogen Adsorption. *Colloids Surf., A* **2020**, *604*, 125303.
(66) Xu, W.; Ferain, E.; Demoustier-Champagne, S.; Glinel, K.; Jonas, A. Hydrogen-Bonded Multilayers for the Release of Polyelectrolyte Nanotubes in Biocompatible Conditions. *ACS Appl. Polym. Mater.* **2019**, *1*, 2407−2416.
(67) Ma, Y.; Sun, J.; Shen, J. Ion-Triggered Exfoliation of Layer-by-Layer Assembled Poly(Acrylic Acid)/Poly(Allylamine Hydrochloride) Films From Substrates: A Facile Way to Prepare Free-Standing Multilayer Films. *Chem. Mater.* **2007**, *19*, 5058−5062.
(68) Zhuk, A.; Pavlukhina, S.; Sukhishvili, S. Hydrogen-Bonded Layer-by-Layer Temperature-Triggered Release Films. *Langmuir* **2009**, *25*, 14025−14029.
(69) Gao, G.; Donath, E.; Moya, S.; Dudnik, V.; Möhwald, H. Elasticity of hollow polyelectrolyte capsules prepared by the layer-by-layer technique. *Eur. Phys. J. E* **2001**, *5*, 21−27.
(70) Anselmo, C.; Zhang, M.; Kumar, S.; Vogus, D. R.; Menegatti, S.; Helgeson, M. E.; Mitragotri, S. Elasticity of nanoparticles influences their blood circulation, phagocytosis, endocytosis, and targeting. *ACS Nano* **2015**, *9*, 3169−3177.
(71) Guo, P.; Liu, D.; Subramanyam, K.; Wang, B.; Yang, J.; Huang, J.; Auguste, D. T.; Moses, M. A. Nanoparticle elasticity directs tumor uptake. *Nat. Commun.* **2018**, *9*, 130.
(72) Kozlovskaya, V.; Alexander, J.; Wang, Y.; Kuncewicz, T.; Liu, X.; Godin, B.; Kharlampieva, E. Internalization of red blood cell-mimicking hydrogel capsules with pH-triggered shape responses. *ACS Nano* **2014**, *8*, 5725−5737.
(73) Kozlovskaya, V.; Xue, B.; Dolmat, M.; Kharlampieva, E. Complete pH-Dependent Shape Recovery in Cubical Hydrogel Capsules After Large Osmotic Deformations. *Macromolecules* **2021**, *54*, 9712−9723.
(74) Kozlovskaya, V.; Higgins, W.; Chen, J.; Kharlampieva, E. Switching Shape of Layer-by-layer Hydrogel Microcontainers. *Chem. Commun.* **2011**, *47*, 8352−8354.
(75) Kozlovskaya, V.; Chen, J.; Tedjo, C.; Liang, X.; Campos-Gomez, J.; Oh, J.; Saeed, M.; Lungu, C. T.; Kharlampieva, E. pH-Responsive Hydrogel Cubes for Release of Doxorubicin in Cancer Cells. *J. Mater. Chem. B* **2014**, *2*, 2494−2507.
(76) Xue, B.; Kozlovskaya; Liu, F.; Chen, J.; Williams, J.; Campos-Gomez, J.; Saeed, M.; Kharlampieva, E. Intracellular degradable hydrogel cubes and spheres for anticancer drug delivery. *ACS Appl. Mater. Interfaces* **2015**, *7*, 13633−13644.
(77) Xue, B.; Wang, W.; Qin, J.-J.; Nijampatnam, B.; Murugesan, S.; Kozlovskaya, V.; Zhang, R.; Velu, S. E.; Kharlampieva, E. Highly efficient delivery of potent anticancer iminoquinone derivative by multilayer hydrogel cubes. *Acta Biomater.* **2017**, *58*, 386−398.
(78) Xue, B.; Kozlovskaya, V.; Sherwani, M. A.; Ratnayaka, S.; Habib, S.; Anderson, T.; Manuvakhova, M.; Klampfer, L.; Yusuf, N.; Kharlampieva, E. Peptide-functionalized Hydrogel Cubes for Active Tumor Targeting. *Biomacromolecules* **2018**, *19*, 4084−4097.
(79) Zyuzin, M. V.; Timin, A. S.; Sukhorukov, G. B. Multilayer Capsules Inside Biological Systems: State-of-the-Art and Open Challenges. *Langmuir* **2019**, *35*, 4747−4762.
(80) Monge, C.; Almodóvar, J.; Boudou, T.; Picart, C. Spatio-temporal Control of LbL Films for Biomedical Applications: From 2D to 3D. *Adv. Healthcare Mater.* **2015**, *4*, 811−830.
(81) Kozlovskaya, V.; Xue, B.; Kharlampieva, E. Shape-Adaptable Polymeric Particles for Controlled Delivery. *Macromolecules* **2016**, *49*, 8373−8386.
(82) Schmitt, J.; Grünewald, T.; Decher, G.; Pershan, P. S.; Kjaer, K.; Lösche, M. Internal Structure of Layer-by-Layer Adsorbed Polyelectrolyte Films: A Neutron and X-ray Reflectivity Study. *Macromolecules* **1993**, *26*, 7058−7063.

https://doi.org/10.1021/acs.langmuir.2c00630
Langmuir XXXX, XXX, XXX−XXX

(83) Ghoussoub, Y. E.; Zerball, M.; Fares, H. M.; Ankner, J. F.; von Klitzing, R.; Schlenoff, J. B. Ion Distribution in Dry Polyelectrolyte Multilayers: A Neutron Reflectometry Study. *Soft Matter* **2018**, *14*, 1699−1708.
(84) Singh, S.; Junghans, A.; Watkins, E.; Kapoor, Y.; Toomey, R.; Majewski, J. Effect of Fluid Shear Stress on Polyelectrolyte Multilayers by Neutron Scatttering Studies. *Langmuir* **2015**, *31*, 2870−2878.
(85) Kellogg, G. J.; Mayes, A. M.; Stockton, W. B.; Ferreira, M.; Rubner, M. F.; Satija, S. K. Neutron Reflectivity Investigations of Self-Assembled Conjugated Polyion Multilayers. *Langmuir* **1996**, *12*, 5109−5113.
(86) v. Klitzing, R. Internal Structure of Polyelectrolyte Multilayer Assemblies. *Phys. Chem. Chem. Phys.* **2006**, *8*, 5012−5033.
(87) Sun, X.; Agate, S.; Salem, K. S.; Lucia, L.; Pal, L. Hydrogel-Based Sensor Networks: Compositions, Properties, and Applications -A Review. *ACS Appl. Bio Mater.* **2021**, *4*, 140−162.
(88) Zhuk, A.; Selin, V.; Zhuk, I.; Belov, B.; Ankner, J. F.; Sukhishvili, S. A. Chain Conformation and Dynamics in Spin-Assisted Weak Polyelectrolyte Multilayers. *Langmuir* **2015**, *31*, 3889−3896.
(89) Jang, Y.; Seo, J.; Akgun, B.; Satija, S.; Char, K. Molecular Weight Dependence on the Disintegration of Spin-Assisted Weak Polyelectrolyte Multilayer Films. *Macromolecules* **2013**, *46*, 4580−4588.
(90) Sill, A.; Nestler, P.; Weltmeyer, A.; Paßvogel, M.; Neuber, S.; Helm, C. A. Polyelectrolyte Multilayer Films from Mixtures of Polyanions: Different Compositions in Films and Deposition Solutions. *Macromolecules* **2020**, *53*, 7107−7118.
(91) Kharlampieva, E.; Kozlovskaya, V.; Ankner, J. F.; Sukhishvili, S. A. Hydrogen-Bonded Polymer Multilayers Probed by Neutron Reflectivity. *Langmiur* **2008**, *24*, 11346−11349.
(92) Wallet, B.; Kharlampieva, E.; Campbell-Proszowska, K. L.; Kozlovskaya, V.; Malak, S.; Ankner, J. F.; Kaplan, D. L.; Tsukruk, V. V. Silk Layering As Studied with Neutron Reflectivity. *Langmuir* **2012**, *28*, 11481−11489.
(93) Kozlovskaya, V.; Ankner, J. F.; O'Neill, H.; Zhang, Q.; Kharlampieva, E. Localized Entrapment of Green Fluorescent Protein Within Nanostructured Polymer Films. *Soft Matter* **2011**, *7*, 11453−11463.
(94) Lösche, M.; Schmitt, J.; Decher, G.; Bouwman, W. G.; Kjaer, K. Detailed Structure of Molecularly Thin Polyelectrolyte Multilayer Films on Solid Substrates as Revealed by Neutron reflectometry. *Macromolecules* **1998**, *31*, 8893−8906.
(95) Jomaa, H. W.; Schlenoff, J. B. Salt-Induced Polyelectrolyte Interdiffusion in Multilayered Films: A Neutron Reflectivity Study. *Macromolecules* **2005**, *38*, 8473−8480.
(96) Kharlampieva, E.; Kozlovskaya, V.; Chan, J.; Ankner, J. F.; Tsukruk, V. V. Spin-Assisted Layer-by-Layer Assembly: Variation of Stratification as Studied with Neutron Reflectivity. *Langmuir* **2009**, *25*, 14017−14024.
(97) Selin, V.; Aliakseyeu, A.; Ankner, J. F.; Sukhishvili, S. A. Effect of a Competitive Solvent on Binding Enthalpy and Chain Intermixing in Hydrogen-Bonded Layer-by-Layer Films. *Macromolecules* **2019**, *52*, 4432−4440.
(98) Sill, A.; Nestler, P.; Azinfar, A.; Helm, C. A. Tailorable Polyanion Diffusion Coefficient in LbL Films: The Role of Polycation Molecular Weight and Polymer Conformation. *Macromolecules* **2019**, *52*, 9045−9052.
(99) Schmitt, J.; Grünewald, T.; Decher, G.; Pershan, P. S.; Kjaer, K.; Lösche, M. *Macromolecules* **1993**, *26*, 7058−7063.
(100) Hamilton, W. A.; Smith, G. S.; Alcantar, N. A.; Majewski, J.; Toomey, R. G.; Kuhl, T. L. Determining the Density Profile of Confined Polymer Brushes with Neutron Reflectivity. *J. Polym. Sci.B: Polym. Phys.* **2004**, *42*, 3290−3301.
(101) Félix, O.; Zheng, Z.; Cousin, F.; Decher, G. Are Sprayed LbL Films Stratified? A First Assessment of the Nanostructure of Spray-Assembled Multilayers by Neutron Reflectometry. *C. R. Chim.* **2009**, *12*, 225−234.
(102) Nolte, A.; Rubner, M.; Cohen, R. Determining the Young's Modulus of Polyelectrolyte Multilayer Films via Stress-Induced Mechanical Buckling Instabilities. *Macromolecules* **2005**, *38*, 5367−5370.
(103) Lisunova, M. O.; Drachuk, I.; Shchepelina, O. A.; Anderson, K. D.; Tsukruk, V. V. Direct Probing of Micromechanical Properties of Hydrogen-Bonded Layer-by-Layer Microcapsule Shells with Different Chemical Compositions. *Langmuir* **2011**, *27*, 11157−11165.
(104) Liu, J.; Chinga-Carrasco, G.; Cheng, F.; Xu, W.; Willfor, S.; Syverud, K.; Xu, C. Hemicellulose-Reinforced Nanocellulose Hydrogels for Wound Healing Application. *Cellulose* **2016**, *23*, 3129−3143.
(105) Mano, J. Viscoelastic Properties of Chitosan with Different Hydration Degrees as Studied by Dynamic Mechanical Analysis. *Macromol. Biosci.* **2008**, *8*, 69−76.
(106) Pavoor, P.; Bellare, A.; Strom, A.; Yang, D.; Cohen, R. Mechanical Characterization of Polyelectrolyte Multilayers Using Quasi-Static Nanoindentation. *Macromolecules* **2004**, *37*, 4865−4871.
(107) Best, J. P.; Javed, S.; Richardson, J. J.; Cho, K. L.; Kamphuis, M. M. J.; Caruso, F. Stiffness-Mediated Adhesion of Cervical Cancer Cells to Soft Hydrogel Films. *Soft Matter* **2013**, *9*, 4580−4584.
(108) Li, H.; Yang, P.; Pageni, P.; Tang, C. Recent Advances in Metal-Containing Polymer Hydrogels. *Macromol. Rapid Commun.* **2017**, *38*, 1700109.
(109) Ejima, H.; Yanai, N.; Best, J. P.; Sindoro, M.; Granick, S.; Caruso, F. Near-incompressible faceted polymer microcapsules from metal-organic framework templates. *Adv. Mater.* **2013**, *25*, 5767−5771.
(110) Shchepelina, O.; Kozlovskaya, V.; Kharlampieva, E.; Mao, W.; Alexeev, A.; Tsukruk, V. V. Anisotropic Micro- and Nano-Capsules. *Macromol. Rapid Commun.* **2010**, *31*, 2041−2046.
(111) Guo, Q.; He, Z.; Jin, Y.; Zhang, S.; Wu, S.; Bai, G.; Xue, H.; Liu, Z.; Jin, S.; Zhao, L.; Wang, J. Tuning Ice Nucleation And Propagation With Counterions On Multilayer Hydrogels. *Langmuir* **2018**, *34*, 11986−11991.
(112) Yang, F.; Hlushko, R.; Wu, D.; Sukhishvili, S.; Du, H.; Tian, F. Ocean Salinity Sensing Using Long-Period Fiber Gratings Functionalized with Layer-By-Layer Hydrogels. *ACS Omega* **2019**, *4*, 2134−2141.
(113) Zhang, X.; Lou, Z.; Yang, X.; Chen, Q.; Chen, K.; Feng, C.; Qi, J.; Luo, Y.; Zhang, D. Fabrication And Characterization Of A Multilayer Hydrogel As A Candidate For Artificial Cartilage. *ACS Appl. Polym. Materials* **2021**, *3*, 5039−5050.
(114) Son, K.; Shin, D.; Kwa, T.; Gao, Y.; Revzin, A. Micropatterned sensing hydrogels integrated with reconfigurable microfluidics for detecting protease release from cells. *Anal. Chem.* **2013**, *85* (24), 11893−11901.
(115) Fan, L.; Xie, J.; Zheng, Y.; Wei, D.; Yao, D.; Zhang, J.; Zhang, T. Antibacterial, self-adhesive, recyclable, and tough conductive composite hydrogels for ultrasensitive strain sensing. *ACS Appl. Mater. Interfaces* **2020**, *12* (19), 22225−22236.
(116) Tang, R.; Meng, Q.; Wang, Z.; Lu, C.; Zhang, M.; Li, C.; Li, Y.; Shen, X.; Sun, Q. Multifunctional ternary hybrid hydrogel sensor prepared via the synergistic stabilization effect. *ACS Appl. Mater. Interfaces* **2021**, *13* (48), 57725−57734.
(117) Jiang, X.; Wang, H.; Yuan, R.; Chai, Y. Functional three-dimensional porous conductive polymer hydrogels for sensitive electrochemiluminescence in situ detection of H_2O_2 released from live cells. *Anal. Chem.* **2018**, *90* (14), 8462−8469.
(118) Chen, Q.; Wang, S.; Huang, T.; Xiao, F.; Wu, Z.; Yu, R. Construction and research of multiple stimuli-responsive 2D photonic crystal DNA hydrogel sensing platform with double-network structure and signal self-expression. *Anal. Chem.* **2022**, *94* (14), 5530−5537.
(119) Lee, M.; Jayathilake, K.; Dai, J.; Meltzer, H. Decreased plasma tryptophan and tryptophan/large neutral amino acid ratio in patients with neuroleptic-resistant schizophrenia: relationship to plasma cortisol concentration. *Psychiatry Res.* **2011**, *185* (3), 328−333.
(120) Van der Heijden, F. M.; Fekkes, D.; Tuinier, S.; Sijben, A. E.; Kahn, R. S.; Verhoeven, W. M. Amino acids in schizophrenia: evidence for lower tryptophan availability during treatment with atypical antipsychotics? *J. Neural Transm.* **2005**, *112*, 577−585.

https://doi.org/10.1021/acs.langmuir.2c00630
Langmuir XXXX, XXX, XXX−XXX

(121) Wu, H.; Tian, C.; Zhang, Y.; Yang, C.; Zhang, S.; Jiang, Z. Stereoselective assembly of amino acid-based metal-biomolecule nanofibers. *Chem. Commun.* **2015**, *51*, 6329−6332.
(122) Remko, M.; Fitz, D.; Rode, B. Effect of metal ions (Li^+, Na^+, K^+, Mg^{2+}, Ca^{2+}, Ni^{2+}, Cu^{2+} and Zn^{2+}) and water coordination on the structure and properties of L-histidine and zwitterionic L-histidine. *Amino Acids* **2010**, *39* (5), 1309−1319.
(123) He, G.; Yan, N.; Cui, H.; Liu, T.; Ding, L.; Fang, Y. A quinoliene-containing conjugated polymer-based sensing platform for amino acids. *Macromolecules* **2011**, *44*, 7096−7099.
(124) Zeng, Q.; Zhang, L.; Li, Z.; Qin, J.; Tang, B. Z. New polyacetylene-based chemosensory materials for the "turn-on" sensing of a-amino acids. *Polymer* **2009**, *50*, 434−440.
(125) Zavgorodnya, O.; Kozlovskaya, V.; Kharlampieva, E. Nano-structured highly-swollen hydrogels: Complexation with amino acids through copper (II) ions. *Polymer* **2015**, *74*, 94−107.
(126) Zavgorodnya, O.; Carmona-Moran, C.; Kozlovskaya, V.; Liu, F.; Wick, T.; Kharlampieva, E. Temperature-Responsive Nanogel Multilayers Of Poly(N-Vinylcaprolactam) For Topical Drug Delivery. *J. Colloid Interface Sci.* **2017**, *506*, 589−602.
(127) Kozlovskaya, V.; Chen, J.; Zavgorodnya, O.; Hasan, M. B.; Kharlampieva, E. Multilayer Hydrogel Capsules with Interpenetrated Network Shell for Encapsulation of Small Molecules. *Langmuir* **2018**, *34*, 11832−11842.
(128) Bauhuber, S.; Hozsa, C.; Breunig, M.; Göpferich, A. Delivery of nucleic acids via disulfide-based carrier systems. *Adv. Mater.* **2009**, *21*, 3286−3306.
(129) Biffi, G.; Tannahill, D.; McCafferty, J.; Balasubramanian, S. Quantitative visualization of DNA g-quadruplex structures in human cells. *Nat. Chem.* **2013**, *5*, 182−186.
(130) Alford, A.; Tucker, B.; Kozlovskaya, V.; Chen, J.; Gupta, N.; Caviedes, R.; Gearhart, J.; Graves, D.; Kharlampieva, E. Encapsulation and Ultrasound-Triggered Release of G-quadruplex DNA in Multilayer Hydrogel Microcapsules. *Polymers* **2018**, *10*, 1342.

https://doi.org/10.1021/acs.langmuir.2c00630
Langmuir XXXX, XXX, XXX−XXX